Drivers of surface salinity changes in the Greenland-Iceland Seas on seasonal and interannual time scales – a climate model study

H.R. Langehaug[1,2], A. Brakstad[2], K. Våge[2], E. Jeansson[3], M. Ilıcak[3,4], C.A. Katsman[5]

[1]Nansen Environmental and Remote Sensing Center, and Bjerknes Centre for Climate Research, Thormøhlensgate 47, 5006 Bergen, Norway
[2]Geophysical Institute, University of Bergen and Bjerknes Centre for Climate Research, Allégaten 70, 5007 Bergen, Norway
[3]NORCE Norwegian Research Centre, Bjerknes Centre for Climate Research, Jahnebakken 5, 5007, Bergen, Norway
[4]Eurasia Institute of Earth Sciences, Istanbul Technical University, Istanbul, Turkey
[5]Department of Hydraulic Engineering, Delft University of Technology, Civil Engineering and Geosciences, Environmental Fluid Mechanics, Delft, Netherlands

Key Points:

- Lateral shifts in the Polar Front occur along all of east Greenland controlled largely by seasonal changes in the westward Ekman transport
- 41 percent of the solid freshwater transport in Fram Strait is diverted from the East Greenland Current into the interior Nordic Seas
- Interannual changes in the solid freshwater diversion is a key driver for surface salinity changes in the Greenland and Iceland Seas

Corresponding author: Helene Reinertsen Langehaug, helene.langehaug@nersc.no

Abstract

The Arctic climate is changing dramatically, especially in terms of sea ice loss, with potentially large downstream impacts on the Nordic Seas and the North Atlantic Ocean. The East Greenland Current (EGC) transports substantial amounts of freshwater (in liquid and solid states) southward along the east Greenland continental slope. To increase our understanding of the drivers of surface salinity changes in the interior Nordic Seas, we investigate the diversion of freshwater from the EGC into the Nordic Seas. To this end, we analyse the outcomes of an ocean model hindcast for the period 1973-2004 with a horizontal resolution of 0.25 degree. We find that sea ice contributes large amounts of freshwater to the interior Nordic Seas. On an interannual time scale, this sea ice diversion has a high and significant correlation with surface salinity in the Greenland and Iceland Seas (correlation < -0.7). On a seasonal time scale, the model hindcast and observations demonstrate a clear signal in surface salinity: a lateral migration of the Polar Front position occurring along all of east Greenland. In the model hindcast, these lateral shifts in the front are consistent with seasonal changes in the westward wind-driven Ekman transport. Thus, this climate model study indicates that there are two main causes of seasonal and interannual surface salinity changes; wind-driven Ekman transport and sea ice diversion from the EGC, respectively.

Plain Language Summary

The main export pathway of freshwater from the Arctic Ocean to the North Atlantic Ocean is the East Greenland Current that flows southward along the east Greenland continental slope. The freshwater is transported both in liquid and solid (as sea ice) states. In this study, we use a global climate model to investigate freshwater diversion from the East Greenland Current and find that 41% of the sea ice export through Fram Strait melts in the interior Nordic Seas. This freshwater inflow may substantially impact where and how much dense water is formed. On an interannual time scale, the model results suggest that this sea ice diversion is an important regulator for the surface salinity across the western Nordic Seas. On a seasonal time scale, large-scale surface salinity changes in the western Nordic Seas are controlled by another process, namely wind-driven westward transport in the upper layers of the ocean.

1 Introduction

One of the main exits of freshwater from the Arctic Ocean is via the western part of Fram Strait, both on the shallow east Greenland shelf and via the East Greenland Current (EGC), which is tied to the shelf break (Fig. 1, e.g., Håvik et al., 2017). The freshwater is transported in the ocean either in liquid or in solid phase (as sea ice). The impact of freshwater can be substantial in key dense-water formation regions, such as the Greenland and Iceland Seas, as it may reduce the depth and density of winter convection and thereby affect the ocean circulation (e.g., Ikeda et al., 2001; Brakstad et al., 2019). The impact of freshwater on the large-scale ocean circulation has been investigated in a number of studies, especially because of the possible future weakening of the meridional overturning circulation in the Atlantic Ocean (Weijer et al., 2020) resulting from an additional freshwater input at high latitudes (e.g., IPCC, 2019; Ionita et al., 2016; Sgubin et al., 2017). However, the impact that increased freshwater input in the Nordic Seas may have on the circulation is highly dependent on *where* it is geographically distributed (Lambert et al., 2016, 2018).

In this study, we focus on mechanisms or processes that divert freshwater from the EGC into the western Nordic Seas in a climate model. Both the solid and liquid freshwater transports through Fram Strait are potential sources of freshwater in the Nordic Seas. Dodd et al. (2009) found, using tracers (salinity, oxygen isotope ratio, and dissolved barium concentration), that a significant amount (80%) of the sea ice exported through

Fram Strait escapes into the interior Nordic Seas. In the Labrador Sea, mechanisms by which freshwater can be transported from the boundary current to the interior have recently been investigated. There coastal upwelling winds play an important role in transporting freshwater away from the coast (Schulze Chretien & Frajka-Williams, 2018; Castelao et al., 2019). Here we investigate in particular the relation between variations in winds, the associated Ekman transport and the surface salinity in the Greenland and Iceland Seas for a relatively long time period (1973-2004). Based on observations, it has been suggested that seasonal variability in the onshore Ekman transport in the western Iceland Sea regulate the location of the Polar Front, which subsequently impacts ventilation in this region (Våge et al., 2018). A recent high-resolution modelling study also found a strong relation between winds and salinity changes in the Greenland Sea, and that such changes occur also on a shorter time scale than the seasonal cycle (Spall et al., 2021). In the present study, we focus also on longer time scales and explore how variations in both winds, through Ekman transport, and sea ice impact salinity variations in the Greenland and Iceland Seas, using a 32-year long climate model simulation. With a better understanding of the mechanisms that divert freshwater into the interior Nordic Seas, we can better predict future changes in key dense-water formation regions, and potentially subsequent changes in the overturning circulation.

The solid freshwater transport through Fram Strait brings substantial amounts of freshwater southward (e.g., Smedsrud et al., 2008). Annually, about 10% of the sea ice area within the Arctic Basin is exported via this route; the sea ice export through the other Arctic gateways is an order of magnitude smaller (Kwok, 2009). The ice export is largely driven by local winds (Vinje, 2001). Exploiting the fact that there is a high correlation between wind and sea ice area export in Fram Strait, the annual mean sea ice area export was estimated to $0.75*10^6$ km^2/year for the period 1957-2005 using NCEP data (Langehaug et al., 2013). In the 1990s the mean sea ice thickness in Fram Strait was 3.4 m (Hansen et al., 2013). Using this thickness, the annual mean sea ice export in Fram Strait is estimated as 62 mSv (1 mSv = $1x10^3$ m^3/s) of freshwater, slightly higher than the estimate for the period 2000-2010 (60 mSv; Haine et al., 2015). The solid freshwater transport through Denmark Strait is much lower than that through Fram Strait, amounting to less than 20 mSv according to a high-resolution modelling study (Behrens et al., 2017).

A substantial amount of liquid freshwater is also carried southward with the EGC. The liquid freshwater in Fram Strait has been monitored over several decades. The long-term annual mean is about 69 mSv (Karpouzoglou et al., 2022). Thus, the solid and liquid freshwater transports are almost equal in magnitude in Fram Strait. In Denmark Strait, the liquid freshwater transport has been estimated to 94 mSv, based on an 11-month mooring record just north of the strait (de Steur et al., 2017). This showed a large variability in the freshwater transport over the year, where values in fall were found to be higher than 170 mSv (de Steur et al., 2017). The increase in liquid freshwater transport between the two straits, in the downstream direction, seems to suggest that most of the liquid freshwater transport in Fram Strait feeds into Denmark Strait. The liquid freshwater transport in Denmark Strait is further strengthened by a sizeable amount of freshwater originating from sea ice melt between the two straits (Dodd et al., 2009). How much freshwater does reach the interior Nordic Seas? The studies above may imply that little liquid freshwater from Fram Strait enters into the interior Nordic Seas. Whether this is indeed the case is the focus of the present study; we investigate primarily how solid freshwater and wind influence salinity in the Greenland and Iceland Sea. We note that ocean currents and eddies can also bring liquid freshwater from the EGC into the interior Nordic Seas. It has been estimated that approximately 10 mSv of freshwater flows eastward with the Jan Mayen Current (Dickson et al., 2007), while 3.4 mSv is carried southeastward with the East Icelandic Current (Macrander et al., 2014). The latter value is the annual mean over a 10-year period (2002-2012). These narrow currents and eddies, neither of which are properly resolved by the model, are not a focus in this study, but we discuss

results from a high-resolution model in the Nordic Seas to better understand the exchange of liquid freshwater from the shelf to the interior (Spall et al., 2021).

Dense-water formation in the Greenland and Iceland Seas has been studied for a long time (e.g., Helland-Hansen and Nansen 1909, Swift & Aagaard, 1981; Karstensen et al., 2005; Våge et al., 2015; Brakstad et al., 2019). The dense water formed in the Nordic Seas is an important source to the large-scale Atlantic Meridional Overturning Circulation (e.g., Chafik & Rossby, 2019), as a substantial part of the dense water spilling across the Greenland-Scotland Ridge on either side of Iceland likely originates in the Greenland and Iceland Seas (e.g., Olsson et al., 2005; Jeansson et al., 2008; Eldevik et al., 2009; Mastropole et al., 2017). In this study, we are not investigating dense-water formation itself in detail. Rather, we focus on how freshwater diversion impacts changes in surface salinity in the Greenland and Iceland Sea. As Brakstad et al. (2019) showed, in this region surface salinity exerts substantial influence on dense-water formation.

As global climate models are frequently used to explore both regional near-term climate predictions and long-term future projections in the Atlantic-Arctic region (e.g., Weijer et al., 2020; Khosravi et al., 2022), it is important to assess how these relatively coarse-resolution models represent key features (e.g., large-scale ocean circulation, sea ice transports, wind forcing) in this region. However, the western Nordic Seas is challenging to study both numerically and observationally. Numerically it is challenging because of the small Rossby radius of deformation (4-5km; Nurser & Bacon, 2014), which implies that 1/25°-resolution model is needed to properly resolve eddy activity in the western Nordic Seas (Hallberg, 2013). In this study, we use an eddy permitting, 1/4°-resolution, global ocean-sea ice model with realistic atmospheric forcing for the period 1973-2004. In the western Nordic Seas, this resolution (about 25 km) is not high enough to resolve the Rossby radius and associated mesoscale processes. However, the horizontal resolution is better than classical IPCC type climate models with resolution of 1° in the ocean. While instabilities and eddies in the boundary current are clearly important for freshwater diversion into the interior (e.g., Spall et al., 2021), large-scale mechanisms such as wind-driven Ekman transport also matter. These can be investigated at the resolution of climate models. Observationally, the westernmost part of the Nordic Seas is severely under-sampled (e.g., Behrendt et al., 2018) due to its harsh conditions and sea ice cover, especially during winter. Thus, it is to some extent challenging to assess the performance of models in this region. At the same time, models are needed as they can contribute to enhanced understanding of dominant processes or mechanisms. In lack of observational estimates of freshwater diversion from the EGC into the interior, we later discuss results from a recently published study, simulating the Nordic Seas for a seasonal cycle using a high-resolution regional model (2-4km; Spall et al., 2021).

Using the global climate model, we address seasonal and interannual variability of large-scale features in the western Nordic Seas over the 32-year long simulation. This long time span is a great advantage, as it better allows us to identify statistically significant relationships, e.g., between wind forcing and hydrography. In Section 2, we first introduce the model, secondly, we assess the horizontal distribution of large-scale currents, eddy kinetic energy, and salinity in the western Nordic Seas, and finally, we describe how liquid and solid freshwater fluxes are calculated. In Section 3, we first present and evaluate the simulated freshwater transports through Fram Strait and Denmark Strait, then we assess the freshwater diversion into the interior of the Nordic Seas. In Section 4, we investigate the relation between wind forcing and surface salinity in the Greenland and Iceland Seas. We find that increased surface salinity in the Greenland and Iceland Seas is associated with increased westward Ekman transport in the same region, and that these fluctuations have a clear seasonal cycle. On an interannual time scale, we find that increased surface salinity in the Greenland and Iceland Seas is associated with less sea ice entering the interior Nordic Seas. Finally, we discuss the results and draw the main conclusions from this study in Section 5.

2 Model, observations, and methods

2.1 Description of the model simulation

We use the ocean sea-ice components of the Norwegian Earth System Model (NorESM, Bentsen et al., 2013), where the atmospheric component is replaced with realistic inter-annual COREv2 atmospheric forcing (Large & Yeager, 2009) for a 60-yr period (1948-2007). Surface fluxes are calculated using the bulk formulae as described in Large & Yeager (2004; 2009). This 1/4°-resolution version of NorESM has been utilized in previous studies (Guo et al., 2016; Langehaug et al., 2019), but not the current simulation. The main difference in this simulation compared with Langehaug et al. (2019) is that the present simulation includes a sub-grid mesoscale eddy parameterisation.

NorESM was run for one cycle (i.e., 60 years) due to the costly integration of the model. We primarily investigate the last part of the cycle, i.e., the time period 1973-2004 (model years 26-57), to avoid model drift and a salinity outlier at the end of the simulation. In climate models, which integrate on longer time scales, monthly averages are typically saved. From the simulation, we thus consider only monthly mean values.

The ocean component (MICOM, Miami Isopycnic Coordinate Ocean Model) in NorESM uses an Arakawa C-grid in the horizontal and 51 density layers as the vertical coordinate (Bentsen et al., 2013). For a more realistic response to atmospheric forcing, a surface mixed-layer is represented by two model layers, where potential density can evolve freely. The 51 density layers range from $\sigma_2 = 28.202$ to $\sigma_2 = 37.800$ kg/m^3 (σ_2 is potential density referenced to 2000 dbar; Bentsen et al., 2013). The mixed-layer depth in the model is parameterised by a turbulent kinetic energy balance equation based on Oberhuber (1993), extended with parameterised mixed-layer re-stratification according to Fox-Kemper et al. (2008) with a coefficient of 0.06. This represents the amount of sub-mesoscale eddies in a grid cell, where 0.06 is the canonical value given in Fox-Kemper et al. (2008).

The parameterised diapycnal mixing consists of several components: Parameterised shear-induced mixing depends on a two-equation turbulence closure scheme (k-epsilon) with Canuto-A stability function (Ilıcak et al., 2008); a fraction of the energy extracted from the mean flow by bottom drag drives mixing in the lowermost isopycnic layers (Legg et al., 2006); tidal-induced mixing is parameterised according to Simmons et al. (2004); the background mixing is latitude-dependent and vertically constant (Gregg et al., 2003), giving a gradual decrease of diffusivity towards the equator with a value of 105 m^2/s at 30° latitude.

This configuration of NorESM uses the thickness diffusivity parameterisation commonly known as Gent and McWilliams (1990) to remove the available potential energy due to unresolved mesoscale eddies. The thickness diffusivity values are computed using Eden and Greatbatch (2008). Isoneutral diffusion values are set equal to thickness diffusivity values, and they are turned off if the model resolves the Rossby radius of deformation locally (similar to the method described by Hallberg, 2013). NorESM also employs a biharmonic Smagorinsky viscosity operator to damp high-frequency grid noise (Smagorinsky, 1993).

Sea Surface Salinity (SSS) restoring (using World Ocean Atlas climatology) is applied globally to avoid local salinity drift. The restoring is applied with a relaxation time scale of 300 days within the first 50 meters of the water column. This value is considered mild relaxation compared to the CORE2 protocol (Danabasoglu et al., 2014). SSS restoring is turned off if the absolute bias is larger than 0.5.

2.2 Observations

The salinity observations used in this study are described in (Huang et al., 2020). In Fig. 2, we show the surface salinity in the Nordic Seas for the period 1986-2004. The

western Nordic Seas with the Greenland and Iceland Seas is known as the *Arctic domain* and separates the low-salinity Polar Water to the west from the high-salinity Atlantic Water to the east (Helland-Hansen and Nansen, 1909). The *Polar Front* separates the Polar and Arctic water masses (Swift & Aagaard, 1981). Following Swift and Aagaard (1981), we define the Polar Front as the 34.5 isohaline. A seasonal migration of the Polar Front is clearly shown in the observations (black line; Fig. 2). In summer (Jul-Sep), the Polar Front has its easternmost position, while the front shifts towards Greenland in fall and winter (Oct-Mar). In spring (Apr-Jun), the front migrates back to the east. In a recent study, Våge et al. (2018) found that the lateral extent of Polar Water varies seasonally in the northwest Iceland Sea. They hypothesized that these lateral shifts are linked to seasonal changes in wind forcing and Ekman transport. The observations used herein demonstrate, for the first time, that the seasonal east-west migration of the Polar Front occurs not only in the Iceland Sea but along all of east Greenland.

2.3 Evaluation of the model simulation

In terms of surface salinity, NorESM shows large variability in the western Nordic Seas, our focus region, in contrast to the eastern Nordic Seas (Fig. 3). The variance is particularly high in the central Greenland and Iceland Seas during summer (Jul-Sep). The modelled surface salinity is compared with that of observations further below.

First, we address how the general circulation is represented in NorESM (Fig. 4a). In the Nordic Seas the large-scale circulation is cyclonic, and the mid-depth circulation is strongly topographically steered (Nøst & Isachsen, 2003; Voet et al., 2010). Near the surface the EGC transports low-salinity Polar Water from the western Fram Strait to Denmark Strait (e.g., Rudels et al., 2005; Håvik et al., 2017). On the opposite side of the Nordic Seas, the Norwegian Atlantic Current and the West Spitsbergen Current transport saline Atlantic Water northwards (e.g., Mauritzen, 1996; Koszalka et al., 2011).

The EGC is clearly evident in NorESM with its high velocities mostly along the Greenland shelf break (Fig. 4a). Along the 1200m isobath, the simulated mixed-layer velocity is about 15-20cm/s. This is lower than what observations indicate (e.g., Håvik et al. (2017) found the EGC to have a core speed between 20-40cm/s). In NorESM, south of about 75°N, the highest velocities are seen on the Greenland shelf (Fig. 4a), which is contrary to observations, where the velocities peak along the continental shelf break (e.g., Håvik et al., 2017). These differences may be a manifestation of limited horizontal resolution of the model. Note that the model data are long-term averages over the period 1973-2004. However, the representation of the EGC in a 1/4°-resolution (eddy-permitting) global ocean simulation is improved over a 1°-resolution, with a stronger and narrower EGC in the higher resolution version (Marsh et al. (2010); using NEMO, Langehaug et al. (2019); using NorESM).

Secondly, we assess the eddy kinetic energy (EKE) in the model (Fig. 4b). EKE is the kinetic energy of the time-varying component of the velocity field, and thus represents a range of processes from mesoscale to large-scale motions (Martínez-Moreno et al., 2019). As described earlier, the horizontal resolution of NorESM is not high enough to resolve the Rossby radius and associated mesoscale processes in the western Nordic Seas. The EKE from the model therefore likely represents mainly the time-varying component of the large-scale motions. The EKE is often calculated based on sea surface height, but to use sea surface height from satellite data is difficult in the western Nordic Seas due to sea ice (Trodahl & Isachsen, 2018). We therefore compare eddy kinetic energy (EKE) in NorESM with that in a higher resolution model (4 km horizontal resolution; Trodahl & Isachsen, 2018). We define EKE, as in Trodahl & Isachsen (2018): $EKE = 0.5*(u'^2+v'^2)^{0.5}$. In Fig. 4b, we show the simulated EKE calculated from mixed-layer velocities. The simulated EKE uses u' and v' that are monthly velocity anomalies with respect to annual mean velocities. Only monthly velocities are available from the model

to calculate EKE. As a consequence, the EKE that we present here is expected to be lower than if we were to use daily velocities from the model. The simulated pattern of EKE resembles the pattern of EKE based on the 4 km resolution model in Trodahl & Isachsen (2018; their Fig. 2). The highest values in NorESM (around 0.1 m/s) are found between Greenland and Iceland. EKE is also relatively high along the EGC (around 0.05 m/s) and then decreases towards the interior Nordic Seas. However, EKE in our simulation is reduced by a factor of about 2 compared to the higher resolution model. The underestimation of EKE is likely the result of using monthly values and due to the horizontal resolution of the model.

Thirdly, we provide a detailed examination of the salinity differences between NorESM and the observations (Fig. 5). The simulated east-west gradient across the western Nordic Seas differs substantially from the observations, especially during summer (Jul-Sep; Fig. 5). The largest difference between the model and the observations is on the Greenland shelf between Fram Strait and Denmark Strait, with NorESM being too saline (salinity differences of up to 2 in some locations). In winter (Jan-Mar; Fig. 5), the shelf is ice-covered and it is difficult to observe salinity. In the interior Nordic Seas, the simulated salinity agrees much better with the observations. Only in the Iceland Sea and the northern Greenland Sea is the simulated salinity lower by up to 0.8-1 in summer. These differences between the simulated and observed salinities are consistent with a previous study, comparing a range of different CORE forced ocean models (including NorESM) in the Nordic Seas and Arctic Ocean (Ilıcak et al., 2016), that all have low horizontal resolution (typically 1° x 1°). Both the magnitude and the pattern of the model differences that were found is similar to what is seen in Fig. 5, with a generally too saline Greenland shelf, too fresh Nordic Seas interior, and too saline Atlantic Water in the east. This suggests that the typical biases that exist in coarse-resolution models persist in the 1/4°-resolution model used here.

Lastly, we compare the simulated Polar Front with that of observations. Because of the salinity differences of about 0.2 along the continental slope between the model simulation and observations, it is more appropriate to choose the 34.3 isohaline than 34.5 to mark the Polar Front in the model (solid magenta line; Fig. 2). A seasonal migration of the Polar Front is simulated in NorESM. In summer, the Polar Front has its easternmost position, while the front shifts towards Greenland in fall and winter. In spring, the front migrates back to the east. The position of the front in the model is not fully aligned with that of observations, but shows overall a similar seasonal migration (compare the solid magenta and black lines; Fig. 2).

In this study, we are interested in the liquid freshwater diversion from the EGC to the interior Nordic Seas. However, we have seen that the east-west salinity gradient in the model differs substantially from the observed gradient. This might be related to the limited ability of the model to properly represent eddies and ocean currents. At the same time, there are too few observations to provide a reliable quantitative estimate of the liquid freshwater entering the interior. For comparison with our model simulation, we therefore discuss results from a very high-resolution regional model (2-4km; Spall et al., 2021). The Nordic Seas was simulated for one seasonal cycle from 2017-2018. Using daily mean values, they investigated the exchange of salt and heat between the shelf and the interior of the Greenland Sea. More specifically, they quantified how oceanic advection changes the properties of the Greenland Sea basin. Considering the annual mean, they found a small impact along the western boundary of the Greenland Sea basin due to shelf-interior exchange. However, on seasonal time scales they found that oceanic advection has a large impact; increasing the salinity in winter and reducing the salinity in summer. The NorESM results are consistent with this; increased surface salinity in the Greenland Sea during winter is associated with increased westward Ekman transport, and reduced surface salinity in summer is associated with reduced westward Ekman transport. This will be shown in Section 3. Spall et al. (2021) further decomposed the small annual mean oceanic ad-

vection along the western boundary into mean advection and eddy advection. The mean advection was larger than the eddy advection and the two components worked in different directions; the mean advection acted to increase the salinity, whereas the eddy advection acted to decrease it. So, in summary, Spall et al. (2021) showed that seasonal exchanges between the shelf and the interior are large and related to the wind stress, whereas the annual mean exchanges are small. We will come back to this when describing the results from NorESM, considering both seasonal and interannual time scales (see Section 3).

Regarding the liquid freshwater transport in Fram Strait and Denmark Strait, we compare NorESM against estimates based on available observations. We find that the model underestimates the liquid freshwater transports in both of these straits (see Section 3).

2.4 Calculation of the combined liquid and solid freshwater transports

In this study we have chosen to use freshwater transports for two practical purposes: 1) we combine the solid and liquid freshwater transports to look at the total impact of freshwater on the surface conditions in the Greenland and Iceland Seas, and, 2) we compare the liquid freshwater transport in the model with the observed liquid freshwater transport in Fram Strait and Denmark Strait (de Steur et al., 2009, 2017, 2018; Karpouzoglou et al., 2022). Currently, freshwater transports is a topic of debate. It is argued that salinity transports, without the need of a salinity reference value, would give results that is comparable from one study to another. Schauer and Losch (2019) have therefore questioned whether freshwater is useful in understanding changes in the ocean. However, when applying a model, we can check for mass balance in the targeted region to ensure that the budget is closed.

We consider the budget of the total (liquid + solid) freshwater transport (FWT) across the boundaries of the enclosed area (see Section 3), where mass is conserved within. To calculate the liquid freshwater transport, we use a similar definition and the same reference value (34.9) as de Steur et al. (2018). The solid freshwater transport is the sea ice volume transport converted to liquid freshwater transport. More details on the calculations of the freshwater transports are given in the Appendix. In the following, liquid freshwater transport refers to freshwater transport in the ocean, and solid freshwater transport refers to transport of sea ice.

2.5 Sections and budget calculations

We have defined four sections that enclose the EGC (Fig. 1). The sections in Fram Strait and Denmark Strait have similar locations to the moored arrays used by de Steur et al. (2017, 2018). To capture the freshwater diversion into the interior Nordic Seas, we have defined a section that is outside the core of the EGC. The section is located along the base of the Greenland continental slope from Fram Strait to Denmark Strait (defined by mean velocities between 7 and 11 cm/s at locations deeper than 1200m; see Fig. 4a). This section is referred to as the outer EGC section. It ends in the Iceland Sea where the 1200m isobath makes a sharp turn toward the west, just north of the Spar Fracture Zone, which bisects the Kolbeinsey Ridge. The location of the Iceland section is chosen to enclose the region. All sections are aligned with the model grid cells.

The mass transport through Fram Strait is mainly balanced by the combined mass transports through the outer EGC section and Denmark Strait. The mass transport through the Iceland section is very small.

3 Assessing freshwater transport in the western Nordic Seas

In this section, we address the long-term mean and seasonal cycle of the simulated freshwater diversion into the interior Nordic Seas. We compare the long-term mean and seasonal FWT in Fram Strait and Denmark Strait in NorESM with observations.

3.1 Long-term mean freshwater budget

We quantify the total freshwater (liquid + solid) diversion into the interior in NorESM as described in Section 2.3 (across the outer EGC section; Fig. 6). The long-term annual mean for the time period 1973-2004 is 17 mSv out of the domain. The solid freshwater diversion (19 mSv) amounts to 41% of the solid freshwater transport entering through Fram Strait (46.2 mSv). Interestingly, all of the freshwater diverted from the EGC into the interior in the model is sea ice, while the liquid part has a small negative contribution (Fig. 6). This supports the findings of Dodd et al. (2009), that sea ice is the main source of freshwater to the interior Nordic Seas. The NorESM results are also consistent with Spall et al. (2021) for the Greenland Sea, showing that the annual mean exchanges of salt between the shelf and the interior are small (a more detailed description of their results are given in Section 2.2). Across the Iceland section, there is only a small liquid freshwater transport of 1 mSv out of the domain (Fig. 6), into the southern Iceland Sea. The freshwater transport across this section therefore plays a minor role in the overall EGC freshwater budget for this model and is not further discussed.

In NorESM, the solid freshwater transport across Fram Strait is much larger than the liquid component (46.2 mSv compared to 10.3 mSv; Fig. 6). In Denmark Strait, the size of the two components are more comparable (20.1 mSv and 18.6 mSv, respectively; Fig. 6). The liquid freshwater transports across Fram and Denmark Straits have previously been quantified based on observations, and amounts to 70 mSv and 94 mSv (more details are provided in the following paragraphs; Table 1), respectively (de Steur et al., 2017, 2018). Although the model underestimates the long-term annual mean of the liquid freshwater transport, the underestimation is of similar magnitude in the two straits. The low values are likely due to the positive salinity bias in the model (too saline water on the Greenland shelf; Fig. 5). An underestimation of liquid freshwater transport in Fram Strait also appears to be a challenge in ocean reanalyses (both 1 degree and 0.25 degree resolution) and also for a finer scale model with 18km resolution (Fuentes-Franco & Koenigk, 2019; Condron et al., 2009).

The observation-based liquid freshwater transport in Fram Strait has been estimated from velocity and hydrography since 1997 (de Steur et al., 2009). The long-term annual mean liquid freshwater transport for the time period 1998-2008 is about 34 mSv (with a reference salinity of 34.8, de Steur et al., 2009), but this value does not include the liquid freshwater transport on the shelf. de Steur et al. (2009) include the shelf (with use of modelling) in their estimate, yielding 62 mSv for the total liquid freshwater transport. More recent estimates covering the period 2003 to 2015, which include the shelf, give a similar annual mean of about 64 mSv (de Steur et al., 2018). With a reference salinity of 34.9, this gives a value of 70 mSv (Table 1). A recent update gives a value of 68.6 mSv for the period 2003-2019 (Karpouzoglou et al., 2022).

North of Denmark Strait, the observation-based liquid freshwater transport was estimated based on moored velocity and hydrographic measurements from September 2011 to July 2012 (de Steur et al., 2017). The mean over that period was estimated to 94 mSv, which includes a contribution from the shelf of about 20 mSv (Table 1). The liquid freshwater transport in Denmark Strait could have been even larger, as November 2011 was a particularly anomalous month. The observational data indicate that a large eddy passed through the mooring array, which caused a temporary reversal of the flow, and therefore gave a relatively low liquid freshwater transport (de Steur et al., 2017).

In NorESM, the long-term annual mean solid freshwater transport in Fram Strait (46.2 mSv) is also underestimated, but to a much lesser extent than the liquid component. Observational studies find that the solid freshwater transport is expected to be of comparable size to the liquid freshwater transport (Dodd et al., 2009), amounting to about 1900 km^3/year or 60 mSv, where the latter is the equivalent freshwater volume stored in sea ice between 2000 and 2010 using a reference salinity of 34.8 (Haine et al., 2015).

On the other hand, the solid freshwater transport in Denmark Strait (20.1 mSv) may be somewhat overestimated in NorESM. Because we do not have observation-based estimates of the solid freshwater transport in this region, we compare NorESM with results from a higher resolution model (1/20°, Behrens et al., 2017). This model shows similar results as NorESM in Denmark Strait: both models have a total (liquid + solid) freshwater transport of about 39 mSv and both models underestimate the liquid freshwater transport. The reason for the underestimation in the higher resolution model is likely of same origin as in NorESM; a positive salinity bias in the Nordic Seas (Fig. 5). In a more detailed comparison, we find that NorESM has a solid component that contributes with 52% of the total freshwater transport (Fig. 6; averaged over 1973-2004), whereas Behrens et al. (2017) show that the solid component contributes with 43% of the total freshwater transport (averaged over 1960-2009). Based on this comparison, the solid freshwater transport in NorESM may be somewhat overestimated.

A similar amount of sea ice that exits Denmark Strait finds its way into the interior Nordic Seas (19 mSv; Fig. 6). Due to model biases and scarce observations, it is difficult to assess if this value is realistic. However, as the solid freshwater transports in Fram Strait and Denmark Strait are fairly realistic, we further quantify the solid freshwater diversion into the interior in NorESM. To determine where freshwater diverges into the interior, the latitudinal distribution of both the liquid and solid components are shown in Fig. 7. The freshwater diversion has been integrated into bins with a width of one degree of latitude. We find that most of the solid component goes into the Greenland Sea with a peak contribution in the southern part, at 73-74°N, (close to 7 mSv). At the same latitude, the liquid freshwater component is less than 1 mSv. In the northern Iceland Sea (at 70-72°N), both the solid and liquid components are negative (both components are less than 2 mSv). The results from Fig. 7 seem to partly reflect the large-scale circulation in the Greenland and Iceland Seas in NorESM. In the southern Greenland Sea, the upper ocean circulation in NorESM shows relatively weak currents (compared to the EGC) towards the east or southeastward (Fig. 4a). This is consistent with the location of the peak freshwater diversion into the Greenland Sea. Close to Jan Mayen, the upper ocean circulation shows typically a stronger westward component compared to further north (Fig. 4a), consistent with the the total freshwater amount that is negative.

3.2 Seasonal mean freshwater budget

Regarding the liquid freshwater transport in Fram Strait, NorESM shows highest values in fall (maximum in October) and lowest in spring and summer (minimum in July), indicated by the magenta curve in Fig. 8a. This compares well with the seasonal cycle in the observations; de Steur et al. (2018) find that the liquid freshwater transport is highest in late fall (November) and lowest during summer (August). North of Denmark Strait, we also find the timing in the simulated seasonal cycle to be fairly realistic. The highest liquid freshwater transport in NorESM occurs in late fall (October and November; Fig. 8b; magenta curve). After this, the liquid freshwater transport is gradually reduced to almost zero in July. In the observations (de Steur et al., 2017), the highest liquid freshwater transport occurs somewhat earlier; in September and October, which is then followed by a clear reduction from December to July. We emphasize that the NorESM results are averaged over a long time period (32 years; 1973-2004), in contrast to the observational data that were obtained over less than one year (Sep 2011-July 2012). Thus, differences in the timing of the seasonal cycle are expected, as a single seasonal cycle might

differ from one year to another. We find that NorESM has large interannual variability in the seasonal cycle of the freshwater transport (grey error bars; Fig. 8b). In Table 1, we have listed observational studies that estimate liquid freshwater transport. Note that several of these have taken place during summer, likely before the timing of the maximum liquid freshwater transport.

In terms of the solid freshwater transport, the seasonal cycle in NorESM is also fairy realistic. In Fram Strait, we compare the solid freshwater transport in NorESM with observation-based sea ice volume transport shown in Zamani et al. (2019) (the solid freshwater transport is dependent on the sea ice volume transport; see the Appendix). We find that the simulated and observation-based seasonal cycles are fairly similar; the highest solid freshwater transport occurs in winter (Dec-Apr) and the lowest in summer (Jun-Aug; light blue curve in Fig. 8a), same as in Zamani et al. (2019). In Denmark Strait, the seasonal cycle of solid freshwater in NorESM compares fairly well with that shown in Behrens et al. (2017). The highest solid freshwater transport occurs during winter and the lowest during summer (with values close to zero; light blue curve in Fig. 8b).

We further investigate the seasonal cycle of the freshwater diversion into the interior in a similar way as for Fram Strait and Denmark Strait (Fig. 8c). Considering only the uppermost part of the ocean (the mixed-layer; strongly influenced by winds), we find that the liquid freshwater diversion has a seasonal cycle (red dashed line; Fig. 8c). This is further discussed in the following section. The seasonal cycle of the solid freshwater diversion into the interior has a similar structure to that in Fram Strait and Denmark Strait, with highest values during winter and lowest during summer (light blue curve; Fig. 8c). In both the outer EGC section and Denmark Strait, the solid freshwater part is also low during fall (Sep-Oct; Fig. 8b and 8c). Furthermore, the results display substantial interannual variability of the freshwater diversion into the interior, both for the total and solid freshwater diversion (grey and light blue vertical lines, respectively, Fig. 8c).

In summary, we find in NorESM that a substantial amount of solid freshwater is diverted into the interior Nordic Sea. We also find that the simulated seasonal cycles of both the liquid and solid components in Fram Strait and Denmark Strait are fairly well represented. In the following section, we further explore the seasonal variability of SSS in the western Nordic Seas and the interannual variability of the solid freshwater diversion into the interior.

4 Mechanisms controlling freshwater diversion in the western Nordic Seas

In this section, we first investigate if there is a link between the seasonal variability of SSS and the large-scale wind stress in the western Nordic Seas in NorESM. The basis for this investigation is the observation-based study by Våge et al. (2018), who hypothesized that there is a link between the two in the Iceland Sea. Secondly, we examine the interannual relationship between SSS in the western Nordic Seas and the freshwater diversion into the interior in NorESM.

4.1 Seasonal relationship between surface salinity and wind stress

Hydrographic observations demonstrate that the Polar Front migrates laterally on seasonal time scales (black lines in Fig. 2). NorESM simulates a similar seasonal shift in the location of the Polar Front (magenta lines in Fig. 2). It has been hypothesized that these lateral shifts are linked to seasonal changes in the Ekman transport (Våge et al., 2018). In Fig. 9, we show the Ekman transport distance in NorESM, decomposed to its zonal and meridional components in winter (Jan-Mar). The Ekman transport distance is estimated as in Våge et al. (2018), and is defined as follows: $X_E = \frac{\tau}{\rho f h}$, where

τ is the monthly mean wind stress, $\rho = 1025 kg/m^3$ is the reference density of sea water, f is the coriolis parameter, and h is the depth of the Ekman layer (we assume a depth of 50m, same as in Våge et al. (2018)). All variables, except the wind stress, are constants, and the Ekman transport distance is thus proportional to the wind stress. The zonal component of the wind stress results in a substantial westward Ekman transport during winter (Fig. 9a), while the meridional component of the wind stress gives a large southward Ekman transport in the northern part of the Greenland Sea (Fig. 9b). Overall, NorESM shows that the westward Ekman transport is dominating the western Nordic Seas in winter.

We consider only the western Nordic Seas (defined by the box in Fig. 9a) and investigate the link between the Ekman transport distance and SSS. The zonal Ekman transport distance displays pronounced seasonal variability (black curve; Fig. 10a). The variability in the meridional component of the Ekman transport distance is much smaller (magenta curve; Fig. 10a). The zonal component shows that the Ekman transport is westward during the whole year. It is highest during winter (Jan-Mar) and fall (Oct-Dec), and has its minimum in summer (Jul). The seasonal cycle in the zonal Ekman transport distance is strongly correlated to SSS; SSS shows a similar cycle, but delayed by one month (red curve; Fig. 10a).

A cross-correlation, using all monthly data for the period 1973-2004, confirms a statistically significant relationship at one month lag between westward Ekman transport distance and SSS in the western Nordic Seas (black curve; Fig. 10b). Hence, a large westward Ekman transport distance during winter and fall contributes to higher SSS in the western Nordic Seas. And vice versa, a small westward Ekman transport distance during summer contributes to lower SSS. The southward Ekman transport distance shows a weak and non-significant correlation with SSS.

The NorESM results support the hypothesis of Våge et al. (2018); that the seasonal migration of the Polar Front is linked to the westward Ekman transport. During summer (Jul-Sep) the Polar Front is at its easternmost position with weak northerly winds. As the northerly winds intensify in fall and winter, the front and the Polar Water are pushed towards Greenland, and the front is at its westernmost position during winter (Jan-Mar). As the winds relax during spring, the Polar Front moves eastward. As a consequence, SSS in the western Nordic Seas has a pronounced wind-driven seasonality.

4.2 Interannual relationship between surface salinity and freshwater diversion

Analysis of the total freshwater budget in NorESM over the period 1973-2004 demonstrates a general diversion of freshwater into the interior Nordic Seas, but that there are large fluctuations in the annual mean from year to year (black bars; Fig. 11a). The changes in the liquid freshwater component can be of similar magnitude as in the solid freshwater component, and hence, can contribute to changes in the total freshwater diversion (magenta and light blue curves; Fig. 11a). Considering only the uppermost layer (i.e., Polar Surface Water with salinity < 34.4), we find similar changes in the liquid freshwater diversion (dashed line; Fig. 11a). This contribution from the liquid component is different from the seasonal cycle in NorESM, where the total freshwater diversion was clearly dominated by the solid freshwater component (Fig. 8c). In addition, we find that the solid component is always positive, whereas the liquid component changes sign from year to year. When there is a high negative peak in the liquid component (years 1984 and 2000), the total freshwater transport is also negative (i.e., there is a freshwater transport directed towards Greenland). Although the changes in the solid and liquid components can be of similar magnitude, the overall contribution to the total freshwater diversion comes from the solid component. In the following, we address the impact of the solid component on SSS in the western Nordic Seas in NorESM.

In NorESM, the temporal evolution of the solid freshwater diversion into the interior appears to be anti-correlated with SSS in the western Nordic Seas (Fig. 11b); a large diversion of solid freshwater coincides with low SSS. A cross-correlation between the two variables confirms a statistically significant link between solid freshwater diversion and SSS on interannual time scales for the period 1973-2004 (blue curve; Fig. 12). We furthermore find that the solid freshwater diversion is positively and significantly correlated with the southward Ekman transport distance in the western Nordic Seas (grey curve; Fig. 12). The main portion of the solid freshwater diversion enters into the Greenland Sea (light blue curve; Fig. 7) during winter (light blue curve; Fig. 8c). The southward Ekman transport distance is also highest during winter (magenta curve; Fig. 10a) and the highest values are found in the northwestern Greenland Sea (Fig. 9b). This suggests that the interannual variability of the solid freshwater diversion is linked in particular to the southward Ekman transport distance in the region where the EGC flows (along the shelfbreak in the northwestern Greenland Sea).

To investigate the link between the freshwater diversion into the interior and SSS in the western Nordic Seas in more detail, we use a composite analysis technique. We assess only years related to high or low freshwater diversion, i.e., values above (below) half of the standard deviation (Fig. 13). We find 12 years with high freshwater diversion into the interior (blue circles, Fig. 13) and 10 years with either low freshwater diversion or negative freshwater transport (red circles, Fig. 13). Note that we consider the total freshwater transport (same as the black bars, Fig. 11a), as we investigate the combined effects of liquid and solid freshwater on the spatial distribution of SSS. Comparing the latitudinal distribution of total freshwater transport for high and low cases, we find the largest differences in the freshwater diversion occurring in the Greenland Sea (thin grey curves; Fig. 7). In addition, we find relatively large differences close to Jan Mayen, where the total freshwater transport is typically negative.

In NorESM, we find that these large fluctuations in high and low freshwater transports are related to SSS anomalies in a relatively large region across the western Nordic Seas (Fig. 14a and 14b). A high freshwater diversion corresponds to a fresh anomaly in the western Nordic Seas (Fig. 14a). In the opposite case, when the total freshwater diversion is low, the surface of the western Nordic Seas is more saline (Fig. 14b). We show the SSS anomalies in late summer (Jul-Sep), as this season has the highest interannual variability of SSS (Fig. 3). The magnitudes of the anomalies are about half of the standard deviation of SSS (compare Fig. 3 and Fig. 14a/14b). Using annual mean SSS in the composite analysis instead of summer SSS shows a similar pattern as in Fig. 14, but with weaker anomalies.

NorESM demonstrates how freshwater diversion into the interior affects SSS in a region covering most of the western Nordic Seas. The clear relationship between high/low freshwater diversion, especially for the solid component, and fresher/more saline surface water in the western Nordic Seas, suggests that solid freshwater diversion is a key driver for salinity changes in the Greenland and Iceland Seas.

5 Discussion and Conclusions

In this study, we have focused on drivers or mechanisms for surface salinity changes in the western Nordic Seas; the Greenland and Iceland Seas that are influenced by a major outflow from the Arctic Ocean (Fig. 1). Observations are sparse in this region, especially for analysis on interannual time scales. We have used a 1/4°-resolution global ocean-sea ice model (NorESM) with realistic atmospheric forcing for the period 1973-2004. This model represents a typical ocean component of coupled global climate models, although with higher resolution. This allows us to analyse drivers of salinity changes both on seasonal and interannual time scales. However, the model has biases, such as a too saline Greenland shelf between Fram Strait and Denmark Strait, and too fresh Nordic

Seas interior (Fig. 5). This results in an underestimation of the liquid freshwater transports in Fram Strait and Denmark Strait (Table 1). The solid freshwater transport is underestimated to some extent in Fram Strait, but slightly overestimated in Denmark Strait. On the other hand, NorESM shows reasonable results for the seasonal shifts in the surface salinity in the Greenland and Iceland Seas, and the seasonal cycles of both the liquid and solid components in Fram Strait and Denmark Strait are fairly well represented.

Previous studies suggest that some of the liquid and solid freshwater transported by the EGC is diverted into the interior of the Nordic Seas (Dickson et al., 2007; Dodd et al., 2009; de Steur et al., 2015; Latarius et al., 2019). In NorESM, we find that solid freshwater (sea ice volume flux) is the major source of freshwater to the interior (Fig. 6), consistent with the results of Dodd et al. (2009). This result is also consistent with a recent study by Selyuzhenok et al. (2020), showing that the sea ice volume flux into the Greenland Sea is dominating the freshwater budget of the Greenland Sea. The annual mean solid freshwater diversion in NorESM (19 mSv) amounts to 41% of the annual mean solid freshwater transport entering through Fram Strait (46.2 mSv). A recent study using a very high-resolution model in the Nordic Seas (Spall et al., 2021) complements our NorESM results, finding that the annual mean exchange of salt between the shelf and the interior in the Greenland Sea is small (considering both mean advection and eddy advection).

In line with observations, a seasonal migration of the Polar Front is simulated in NorESM (Fig. 2). However, the position of the front is not fully aligned with that of the observations, which can probably be attributed to the limited horizontal resolution of the model. Although our model is relatively coarse, we use the model to test the hypothesis of Våge et al. (2018); that winds regulate the seasonal migration of the Polar Front. Våge et al. (2018) suggested that a westward displacement of the front in the Iceland Sea is caused by increased onshore Ekman transport due to enhanced northerly winds in fall and winter. In our study, we find that the shifts in the Polar Front not only occurs in the Iceland Sea, but all along east Greenland north of Denmark Strait. This is demonstrated both in observations and in NorESM (Fig. 2). NorESM shows a statistically significant relationship (correlation > 0.5 at one month lag) between westward Ekman transport distance and SSS in the western Nordic Seas (Fig. 10b), and thus supports the hypothesis of Våge et al (2018); that the location of the Polar Front is linked to the wind forcing.

On an interannual time scale, NorESM shows that changes in surface salinity in the western Nordic Seas is strongly related to changes in the annual mean solid freshwater diversion (correlation < -0.7, Fig. 12). Such surface salinity changes take place all along east Greenland; an increase in the solid freshwater diversion from the EGC coincides with a negative salinity anomaly in the western Nordic Seas, and visa versa (Fig. 14a and 14b). The solid freshwater diversion is largest in winter (Dec-Apr, Fig. 8c) and the largest salinity anomalies occur in late summer (Jul-Aug-Sep, Fig. 3). This suggests that sea ice reaching the interior Nordic Seas melts there during summer and modifies the surface salinity in late summer.

We find that the main source of sea ice into the interior comes from Fram Strait ice export, although another source could also be locally formed sea ice. The observation-based study of Venegas and Mysak (2000) found that sea ice variability in the Greenland Sea during 1950-1998 was to a large extent explained by variability in ice export through Fram Strait and by local wind anomalies during winter. Consistent with that, in our model simulation we find that the solid freshwater transport through Fram Strait covary to some extent with the diversion into the interior on interannual time scales (correlation of 0.43 at zero time lag).

On even longer time scales, the drivers of salinity changes in this region are suggested to be rooted in the subpolar North Atlantic and decadal changes in the Atlantic inflow into the Nordic Seas (e.g., Glessmer et al., 2014; Lauvset et al., 2018; Kenigson & Timmermans, 2021). Thus, main drivers of salinity changes in the western Nordic Seas appear to depend on the time scales considered; local winds driving seasonal changes, more Arctic-driven interannual changes via sea ice diversion from the EGC, and more Atlantic-driven decadal changes via the Atlantic inflow. The time scales of these different mechanisms give an indication of how far ahead we can predict changes in surface salinity.

Several recent papers demonstrate predictability several years ahead in the upper ocean temperature and salinity in the *eastern* Nordic Seas – or more specifically the Atlantic domain. This predictability is linked to changes in the properties of Atlantic Water farther upstream (Chafik et al., 2015; Årthun et al., 2017; Langehaug et al., 2019), although predictability is limited to some extent by local surface forcing (Asbjørnsen et al., 2019). Changes in the properties of the Atlantic Water also influence the *western* Nordic Seas – in the Arctic and Polar domains (e.g., Eldevik et al., 2009; Årthun & Eldevik, 2016; Lauvset et al., 2018), but the signal is diminished for several reasons, such as mixing with the southward-flowing fresh Polar Water (Håvik et al., 2017). Furthermore, the predictability related to the amount of sea ice and liquid freshwater from the Arctic Ocean is limited, with predictability only one year ahead (Schmith et al., 2018). This is consistent with two studies using dynamical prediction models (Germe et al., 2014; Dai et al., 2020), showing some skill in predicting sea ice extent in the Nordic Seas up to only one year ahead. Thus, the predictability beyond one year of the upper ocean and sea ice in the Polar and Arctic domains appears to be low compared to the predictability in the Atlantic domain.

Appendix A Calculation of liquid freshwater transport

In addition to the freshwater transports, we have also looked at the salinity transports for the same area. The salinity transport gives reasonable values (about 250kt/s) in the western Fram Strait (Schauer & Losch, 2019) and a budget close to balance. The incoming salt transport in Fram Strait is balanced by the outgoing salt transport in the outer EGC and Denmark Strait. The salt transport in the Iceland section is very small due to a very small volume transport.

The liquid freshwater transport (FWTocean) is calculated in each of the sections shown in Fig. 1. This transport has been calculated in a similar way as in previous observational studies of the FWTocean through a section north of Denmark Strait (de Steur et al., 2017) and through the western Fram Strait (de Steur et al., 2009, 2018). In Equation (1), based on the observational studies, V is volume transport in Sv, S is salinity, and the reference salinity ($Sref$) is defined herein as 34.9.

However, in this study, we use Equation (2) for the model output. The model output from NorESM is given as mass flux, Mf (kg/s), and salt flux, Sf (kg/s). We apply Equation (2) because the nonlinear terms in the salt flux of the ocean model is not captured by the formulation $V \times S$ in Equation (1). For an instantaneous moment in time, the two equations are the same (i.e., Sf is equal to $V \times S$). However, the model output is monthly means and monthly Sf does not equal $V \times S$. In Equation (2) we multiply Sf by 1000 kg/m^3, as the modelled Sf has not been multiplied by the density of water during the model run.

$$FWTocean = \int_{x1}^{x2} \int_{z(S=Sref)}^{z=0} V(x,z) \times \frac{Sref - S(x,z)}{Sref} dz dx \tag{1}$$

$$FWTocean = \sum_{x1}^{x2} \sum_{z(S=Sref)}^{z=0} Mf(x,z) - \frac{1000 \times Sf(x,z)}{Sref} \tag{2}$$

In order to compare with observational values, we further divide FWTocean from the model by a density of 1000kg/m^3 to convert to the unit mSv.

In the literature there are studies that calculate the FWTocean as in Equation (2), but without dividing Sf by $Sref$. In this study we want to calculate the FWTocean in a similar way to the observational studies in Fram Strait and Denmark Strait, and therefore we divide by $Sref$.

We have compared the resulting FWTocean of using Equation (1) and Equation (2), and we find that the mean seasonal cycle for the time period 1973-2004 are fairly similar in Denmark Strait (not shown). However, the results are not that similar in Fram Strait, probably because of the more complex ocean circulation in that region. Comparing the resulting interannual variability from the two Equations, we find in general larger variance using Equation (2) and also the timing of the peaks appears to be more realistic compared to the observed FWTocean in Fram Strait (de Steur et al., 2009).

Appendix B Calculation of solid freshwater transport (sea ice volume transport)

The sea ice volume transport, VOLice, is calculated in each of the sections shown in Fig. 1, and the general formula is as in Equation (3).

$$VOLice = hi \times vel \times dx, \tag{3}$$

where hi is the grid cell mean ice thickness (m), vel is the ice velocity (m/s), and dx is size of the grid cell (m).

The sea ice volume transport is converted to a solid freshwater transport, FWTice, according to Equation (4). This formula is given in (Curry et al., 2014).

$$FWTice = VOLice \times \frac{Sref - Sice}{Sref} \times \frac{\rho ice}{\rho water}, \tag{4}$$

where $Sice = 5$ (sea ice salinity), $\rho ice = 900 kg/m^3$ (density of sea ice), and $\rho water = 1000 kg/m^3$ (density of freshwater).

Acknowledgments

The research leading to these results has received funding from the Research Council of Norway (RCN) through the project VENTILATE (229791) (HRL, EJ). This is a contribution to the strategic project FRESHWATER (HRL, KV, EJ) of the Bjerknes Centre for Climate Research. HRL has also been funded by the Blue-Action Project (European Union's Horizon 2020 research and innovation program, Grant 727852). KV and AB were funded by the Trond Mohn Foundation under Grant BFS2016REK01. This study has also been supported by the institutional basic funding to the Nansen Center granted by the Research Council of Norway (project no. 218857). Regarding the production of the model experiment used herein, we thank EVA (Earth system modelling of climate Variations in the Anthropocene) with RCN project number 229771.

Data Availability Statement

Model output from the Bjerknes Centre for Climate Research are archived at Sigma2: The Norwegian e-infrastructure for Research and Education. Information about the model

and the version used is given in Section 2.1. The salinity observations used in this study are described in Huang et al. (2020).

Tables

Table 1. Freshwater transports (only liquid; mSv) in observations and NorESM with the annual mean ($MEAN$) and the maximum value of the mean seasonal cycle (MAX) given below. All values using a reference salinity of 34.9 are marked by a star (*). Otherwise, a reference salinity of 34.8 is used. Most of the observational values include the freshwater transport on the shelf (shown in bold). The model data includes both and cover the period 1973-2004. The maximum value of the simulated seasonal cycle is in October (October and November) in Fram Strait (Denmark Strait).

Strait	$MEAN_{obs}$	MAX_{obs}	$MEAN_{model}$	MAX_{model}
Fram Strait[a]	**70***	>**80***	**10***	**20***
Fram Strait[b]	**68.6***			
Denmark Strait[c]	**94***	>**130***	**19***	**35***
Denmark Strait[d]		**81**		
Denmark Strait[e]		55		
Denmark Strait[f]		43-60*		

[a] Observational values from the period 2003-2015. The maximum value is the November value from Fig. 3d in de Steur et al. (2018).
[b] Observational values are updated for the period 2003-2019 (Karpouzoglou et al., 2022).
[c] Observational values from the period Sep 2011 to Jul 2012. The maximum value is the September value from Fig. 7a in de Steur et al. (2017). They assume a contribution from the shelf (20 mSv).
[d] Observational values from summer (Jul-Aug) 2012 (Håvik et al., 2017, their section 3).
[e] Observational values from summer (Jul-Aug) 2004 (Sutherland & Pickart, 2008).
[f] Observational values from Oct 1998 and Aug 1999 (Dodd et al., 2009).

References

Årthun, M., & Eldevik, T. (2016). On anomalous ocean heat transport toward the arctic and associated climate predictability. *Journal of Climate*, *29*(2), 689-704. Retrieved from http://dx.doi.org/10.1175/JCLI-D-15-0448.1 doi: 10.1175/JCLI-D-15-0448.1

Årthun, M., Eldevik, T., Viste, E., Drange, H., Furevik, T., Johnson, H. L., & Keenlyside, N. S. (2017). Skillful prediction of northern climate provided by the ocean. *Nature Communications*, *8*(1), 15875. Retrieved from https://doi.org/10.1038/ncomms15875 doi: 10.1038/ncomms15875

Asbjørnsen, H., Årthun, M., Skagseth, Ø., & Eldevik, T. (2019). Mechanisms of ocean heat anomalies in the norwegian sea. *Journal of Geophysical Research: Oceans*, *124*(4), 2908-2923. Retrieved from https://agupubs.onlinelibrary.wiley.com/doi/abs/10.1029/2018JC014649 doi: 10.1029/2018JC014649

Behrendt, A., Sumata, H., Rabe, B., & Schauer, U. (2018). Udash - unified database for arctic and subarctic hydrography. *Earth System Science Data*, *10*(2), 1119-1138. Retrieved from https://www.earth-syst-sci-data.net/10/1119/2018/ doi: 10.5194/essd-10-1119-2018

Behrens, E., Våge, K., Harden, B., Biastoch, A., & Böning, C. W. (2017). Composition and variability of the denmark strait overflow water in a high-resolution numerical model hindcast simulation. *Journal of Geophysical Research: Oceans*, *122*(4), 2830-2846. Retrieved from https://agupubs.onlinelibrary.wiley.com/doi/abs/10.1002/2016JC012158 doi: https://doi.org/10.1002/2016JC012158

Bentsen, M., Bethke, I., Debernard, J. B., Iversen, T., Kirkevåg, A., Seland, Ø., ... Kristjánsson, J. E. (2013). The norwegian earth system model, noresm1-m - part 1: Description and basic evaluation of the physical climate. *Geoscientific Model Development*, *6*(3), 687-720. Retrieved from https://www.geosci-model-dev.net/6/687/2013/ doi: 10.5194/gmd-6-687-2013

Brakstad, A., Våge, K., Håvik, L., & Moore, G. W. K. (2019). Water mass transformation in the greenland sea during the period 1986–2016. *Journal of Physical Oceanography*, *49*(1), 121-140. doi: 10.1175/JPO-D-17-0273.1

Castelao, R. M., Luo, H., Oliver, H., Rennermalm, A. K., Tedesco, M., Bracco, A., ... Medeiros, P. M. (2019). Controls on the transport of meltwater from the southern greenland ice sheet in the labrador sea. *Journal of Geophysical Research: Oceans*, *124*(6), 3551-3560. Retrieved from https://agupubs.onlinelibrary.wiley.com/doi/abs/10.1029/2019JC015159 doi: https://doi.org/10.1029/2019JC015159

Chafik, L., Nilsson, J., Skagseth, Ø., & Lundberg, P. (2015). On the flow of atlantic water and temperature anomalies in the nordic seas toward the arctic ocean. *Journal of Geophysical Research: Oceans*, *120*(12), 7897-7918. Retrieved from http://dx.doi.org/10.1002/2015JC011012 doi: 10.1002/2015JC011012

Chafik, L., & Rossby, T. (2019). Volume, heat, and freshwater divergences in the subpolar north atlantic suggest the nordic seas as key to the state of the meridional overturning circulation. *Geophysical Research Letters*, *46*(9), 4799-4808. Retrieved from https://agupubs.onlinelibrary.wiley.com/doi/abs/10.1029/2019GL082110 doi: 10.1029/2019GL082110

Condron, A., Winsor, P., Hill, C., & Menemenlis, D. (2009). Simulated response of the arctic freshwater budget to extreme nao wind forcing. *Journal of Climate*, *22*(9), 2422 - 2437. Retrieved from https://journals.ametsoc.org/view/journals/clim/22/9/2008jcli2626.1.xml doi: 10.1175/2008JCLI2626.1

Curry, B., Lee, C. M., Petrie, B., Moritz, R. E., & Kwok, R. (2014). Multiyear volume, liquid freshwater, and sea ice transports through davis strait, 2004–10. *Journal of Physical Oceanography*, *44*(4), 1244-1266. Retrieved from https://doi.org/10.1175/JPO-D-13-0177.1 doi: 10.1175/JPO-D-13-0177.1

Dai, P., Gao, Y., Counillon, F., Wang, Y., Kimmritz, M., & Langehaug, H. R. (2020). Seasonal to decadal predictions of regional arctic sea ice by assimilating sea surface temperature in the norwegian climate prediction model. *Climate Dynamics*. Retrieved from https://doi.org/10.1007/s00382-020-05196-4 doi: 10.1007/s00382-020-05196-4

Danabasoglu, G., Yeager, S. G., Bailey, D., Behrens, E., Bentsen, M., Bi, D., ... Wang, Q. (2014, 1). North atlantic simulations in coordinated ocean-ice reference experiments phase ii (core-ii). part i: Mean states. *Ocean Modelling*, *73*, 76-107. Retrieved from http://www.sciencedirect.com/science/article/pii/S1463500313001868 doi: http://dx.doi.org/10.1016/j.ocemod.2013.10.005

de Steur, L., Hansen, E., Gerdes, R., Karcher, M., Fahrbach, E., & Holfort, J. (2009). Freshwater fluxes in the east greenland current: A decade of observations. *Geophysical Research Letters*, *36*(23). Retrieved from https://agupubs.onlinelibrary.wiley.com/doi/abs/10.1029/2009GL041278 doi: 10.1029/2009GL041278

de Steur, L., Peralta-Ferriz, C., & Pavlova, O. (2018). Freshwater export in the east greenland current freshens the north atlantic. *Geophysical Research Let-*

ters, *45*(24), 13,359-13,366. doi: 10.1029/2018GL080207

de Steur, L., Pickart, R. S., Macrander, A., Våge, K., Harden, B., Jónsson, S., ... Valdimarsson, H. (2017). Liquid freshwater transport estimates from the east greenland current based on continuous measurements north of denmark strait. *Journal of Geophysical Research: Oceans*, *122*(1), 93-109. doi: 10.1002/2016JC012106

de Steur, L., Pickart, R. S., Torres, D. J., & Valdimarsson, H. (2015). Recent changes in the freshwater composition east of greenland. *Geophysical Research Letters*, *42*(7), 2326-2332. Retrieved from https://agupubs.onlinelibrary.wiley.com/doi/abs/10.1002/2014GL062759 doi: 10.1002/2014GL062759

Dickson, R. R., Rudels, B., Dye, S., Karcher, M., Meincke, J., & Yashayaev, I. (2007). Current estimates of freshwater flux through arctic and subarctic seas. *Progress in Oceanography*, *73*(3), 210 - 230. Retrieved from http://www.sciencedirect.com/science/article/pii/S007966110700081X (Observing and Modelling Ocean Heat and Freshwater Budgets and Transports) doi: https://doi.org/10.1016/j.pocean.2006.12.003

Dodd, P. A., Heywood, K. J., Meredith, M. P., Naveira-Garabato, A. C., Marca, A. D., & Falkner, K. K. (2009). Sources and fate of freshwater exported in the east greenland current. *Geophysical Research Letters*, *36*(19). Retrieved from https://agupubs.onlinelibrary.wiley.com/doi/abs/10.1029/2009GL039663 doi: 10.1029/2009GL039663

Eden, C., & Greatbatch, R. J. (2008). Towards a mesoscale eddy closure. *Ocean Modelling*, *20*(3), 223 - 239. Retrieved from http://www.sciencedirect.com/science/article/pii/S1463500307001163 doi: https://doi.org/10.1016/j.ocemod.2007.09.002

Eldevik, T., Nilsen, J. E. Ø., Iovino, D., Anders Olsson, K., Sandø, A. B., & Drange, H. (2009, 06). Observed sources and variability of nordic seas overflow. *Nature Geosci*, *2*(6), 406-410. Retrieved from http://dx.doi.org/10.1038/ngeo518

Fox-Kemper, B., Ferrari, R., & Hallberg, R. (2008). Parameterization of mixed layer eddies. part i: Theory and diagnosis. *Journal of Physical Oceanography*, *38*(6), 1145-1165. Retrieved from http://dx.doi.org/10.1175/2007JPO3792.1 doi: 10.1175/2007JPO3792.1

Fuentes-Franco, R., & Koenigk, T. (2019). Sensitivity of the arctic freshwater content and transport to model resolution. *Climate Dynamics*, *53*(3), 1765–1781. Retrieved from https://doi.org/10.1007/s00382-019-04735-y doi: 10.1007/s00382-019-04735-y

Gent, P. R., & McWilliams, J. C. (1990). Isopycnal mixing in ocean circulation models. *Journal of Physical Oceanography*, *20*(1), 150-155. Retrieved from http://dx.doi.org/10.1175/1520-0485(1990)020<0150:IMIOCM>2.0.CO;2 doi: 10.1175/1520-0485(1990)020⟨0150:IMIOCM⟩2.0.CO;2

Germe, A., Chevallier, M., Salas y Mélia, D., Sanchez-Gomez, E., & Cassou, C. (2014). Interannual predictability of arctic sea ice in a global climate model: regional contrasts and temporal evolution. *Climate Dynamics*, *43*(9), 2519-2538. Retrieved from https://doi.org/10.1007/s00382-014-2071-2 doi: 10.1007/s00382-014-2071-2

Glessmer, M. S., Eldevik, T., Våge, K., Øie Nilsen, J. E., & Behrens, E. (2014). Atlantic origin of observed and modelled freshwater anomalies in the nordic seas. *Nature Geoscience*, *7*(11), 801–805. Retrieved from https://doi.org/10.1038/ngeo2259 doi: 10.1038/ngeo2259

Gregg, M. C., Sanford, T. B., & Winkel, D. P. (2003). Reduced mixing from the breaking of internal waves in equatorial waters. *Nature*, *422*(6931), 513-515. Retrieved from http://dx.doi.org/10.1038/nature01507

Guo, C., Ilicak, M., Bentsen, M., & Fer, I. (2016). Characteristics of the nordic seas overflows in a set of norwegian earth system model experiments. *Ocean*

Modelling, *104*, 112-128. Retrieved from http://www.sciencedirect.com/science/article/pii/S1463500316300543 doi: http://dx.doi.org/10.1016/j.ocemod.2016.06.004

Haine, T. W., Curry, B., Gerdes, R., Hansen, E., Karcher, M., Lee, C., ... Woodgate, R. (2015). Arctic freshwater export: Status, mechanisms, and prospects. *Global and Planetary Change*, *125*, 13 - 35. doi: https://doi.org/10.1016/j.gloplacha.2014.11.013

Hallberg, R. (2013). Using a resolution function to regulate parameterizations of oceanic mesoscale eddy effects. *Ocean Modelling*, *72*, 92 - 103. Retrieved from http://www.sciencedirect.com/science/article/pii/S1463500313001601 doi: https://doi.org/10.1016/j.ocemod.2013.08.007

Hansen, E., Gerland, S., Granskog, M. A., Pavlova, O., Renner, A. H. H., Haapala, J., ... Tschudi, M. (2013). Thinning of arctic sea ice observed in fram strait: 1990–2011. *Journal of Geophysical Research: Oceans*, *118*(10), 5202-5221. Retrieved from https://agupubs.onlinelibrary.wiley.com/doi/abs/10.1002/jgrc.20393 doi: https://doi.org/10.1002/jgrc.20393

Håvik, L., Pickart, R. S., Våge, K., Torres, D., Thurnherr, A. M., Beszczynska-Möller, A., ... von Appen, W.-J. (2017). Evolution of the east greenland current from fram strait to denmark strait: Synoptic measurements from summer 2012. *Journal of Geophysical Research: Oceans*, *122*(3), 1974-1994. doi: 10.1002/2016JC012228

Huang, J., Pickart, R. S., Huang, R. X., Lin, P., Brakstad, A., & Xu, F. (2020). Sources and upstream pathways of the densest overflow water in the nordic seas. *Nature Communications*, *11*(1), 5389. Retrieved from https://doi.org/10.1038/s41467-020-19050-y doi: 10.1038/s41467-020-19050-y

Ikeda, M., Wang, J., & Zhao, J.-P. (2001). Hypersensitive decadal oscillations in the arctic/subarctic climate. *Geophysical Research Letters*, *28*(7), 1275-1278. Retrieved from https://agupubs.onlinelibrary.wiley.com/doi/abs/10.1029/2000GL011773 doi: https://doi.org/10.1029/2000GL011773

Ilıcak, M., Drange, H., Wang, Q., Gerdes, R., Aksenov, Y., Bailey, D., ... Yeager, S. G. (2016, 4). An assessment of the arctic ocean in a suite of interannual core-ii simulations. part iii: Hydrography and fluxes. *Ocean Modelling*, *100*, 141-161. Retrieved from http://www.sciencedirect.com/science/article/pii/S1463500316000238 doi: http://dx.doi.org/10.1016/j.ocemod.2016.02.004

Ilıcak, M., Özgökmen, T. M., Peters, H., Baumert, H. Z., & Iskandarani, M. (2008). Performance of two-equation turbulence closures in three-dimensional simulations of the red sea overflow. *Ocean Modelling*, *24*(3), 122 - 139. Retrieved from http://www.sciencedirect.com/science/article/pii/S1463500308000838 doi: https://doi.org/10.1016/j.ocemod.2008.06.001

Ionita, M., Scholz, P., Lohmann, G., Dima, M., & Prange, M. (2016). Linkages between atmospheric blocking, sea ice export through fram strait and the atlantic meridional overturning circulation. *Scientific Reports*, *6*(1), 32881. Retrieved from https://doi.org/10.1038/srep32881 doi: 10.1038/srep32881

Jeansson, E., Jutterström, S., Rudels, B., Anderson, L. G., Olsson], K. A., Jones, E. P., ... Swift, J. H. (2008). Sources to the east greenland current and its contribution to the denmark strait overflow. *Progress in Oceanography*, *78*(1), 12 - 28. Retrieved from http://www.sciencedirect.com/science/article/pii/S0079661108000803 doi: https://doi.org/10.1016/j.pocean.2007.08.031

Karpouzoglou, T., de Steur, L., Smedsrud, L. H., & Sumata, H. (2022). Observed changes in the arctic freshwater outflow in fram strait. *Journal of Geophysical Research: Oceans*, *127*(3), e2021JC018122. Retrieved from https://agupubs.onlinelibrary.wiley.com/doi/abs/10.1029/2021JC018122 (e2021JC018122 2021JC018122) doi: https://doi.org/10.1029/2021JC018122

Karstensen, J., Schlosser, P., Wallace, D. W. R., Bullister, J. L., & Blindheim, J.

(2005). Water mass transformation in the greenland sea during the 1990s. *Journal of Geophysical Research: Oceans*, *110*(C7). Retrieved from https://agupubs.onlinelibrary.wiley.com/doi/abs/10.1029/2004JC002510 doi: 10.1029/2004JC002510

Kenigson, J. S., & Timmermans, M.-L. (2021). Nordic seas hydrography in the context of arctic and north atlantic ocean dynamics. *Journal of Physical Oceanography*, *51*(1), 101 - 114. Retrieved from https://journals.ametsoc.org/view/journals/phoc/51/1/jpo-d-20-0071.1.xml doi: 10.1175/JPO-D-20-0071.1

Khosravi, N., Wang, Q., Koldunov, N., Hinrichs, C., Semmler, T., Danilov, S., & Jung, T. (2022). The arctic ocean in cmip6 models: Biases and projected changes in temperature and salinity. *Earth's Future*, *10*(2), e2021EF002282. Retrieved from https://agupubs.onlinelibrary.wiley.com/doi/abs/10.1029/2021EF002282 (e2021EF002282 2021EF002282) doi: https://doi.org/10.1029/2021EF002282

Koszalka, I., LaCasce, J., Andersson, M., Orvik, K., & Mauritzen, C. (2011). Surface circulation in the nordic seas from clustered drifters. *Deep Sea Research Part I: Oceanographic Research Papers*, *58*(4), 468 - 485. Retrieved from http://www.sciencedirect.com/science/article/pii/S0967063711000306 doi: https://doi.org/10.1016/j.dsr.2011.01.007

Kwok, R. (2009). Outflow of arctic ocean sea ice into the greenland and barents seas: 1979–2007. *Journal of Climate*, *22*(9), 2438-2457.

Lambert, E., Eldevik, T., & Haugan, P. M. (2016). How northern freshwater input can stabilise thermohaline circulation. *Tellus A: Dynamic Meteorology and Oceanography*, *68*(1), 31051. doi: 10.3402/tellusa.v68.31051

Lambert, E., Eldevik, T., & Spall, M. A. (2018). On the dynamics and water mass transformation of a boundary current connecting alpha and beta oceans. *Journal of Physical Oceanography*, *48*(10), 2457-2475. doi: 10.1175/JPO-D-17-0186.1

Langehaug, H. R., Geyer, F., Smedsrud, L., & Gao, Y. (2013). Arctic sea ice decline and ice export in the cmip5 historical simulations. *Ocean Modelling*, *71*(0), 114 - 126. doi: http://dx.doi.org/10.1016/j.ocemod.2012.12.006

Langehaug, H. R., Sandø, A. B., Årthun, M., & Ilıcak, M. (2019). Variability along the atlantic water pathway in the forced norwegian earth system model. *Climate Dynamics*, *52*(1), 1211-1230. Retrieved from https://doi.org/10.1007/s00382-018-4184-5 doi: 10.1007/s00382-018-4184-5

Large, W. G., & Yeager, S. G. (2009). The global climatology of an interannually varying air-sea flux data set. *Climate Dynamics*, *33*(2), 341-364. Retrieved from http://dx.doi.org/10.1007/s00382-008-0441-3 doi: 10.1007/s00382-008-0441-3

Latarius, K., Schauer, U., & Wisotzki, A. (2019). Near-ice hydrographic data from seaglider missions in the western greenland sea in summer 2014 and 2015. *Earth System Science Data*, *11*(2), 895-920. Retrieved from https://www.earth-syst-sci-data.net/11/895/2019/ doi: 10.5194/essd-11-895-2019

Lauvset, S. K., Brakstad, A., Våge, K., Olsen, A., Jeansson, E., & Mork, K. A. (2018). Continued warming, salinification and oxygenation of the greenland sea gyre. *Tellus A: Dynamic Meteorology and Oceanography*, *70*(1), 1-9. Retrieved from https://doi.org/10.1080/16000870.2018.1476434 doi: 10.1080/16000870.2018.1476434

Legg, S., Hallberg, R. W., & Girton, J. B. (2006). Comparison of entrainment in overflows simulated by z-coordinate, isopycnal and non-hydrostatic models. *Ocean Modelling*, *11*(1-2), 69-97. Retrieved from http://www.sciencedirect.com/science/article/pii/S1463500304001064 doi: http://dx.doi.org/10.1016/j.ocemod.2004.11.006

Macrander, A., Valdimarsson, H., & Jónsson, S. (2014). Improved transport estimate of the east icelandic current 2002–2012. *Journal of Geophysical Research: Oceans*, *119*(6), 3407-3424. Retrieved from https://agupubs.onlinelibrary.wiley.com/doi/abs/10.1002/2013JC009517 doi: 10.1002/2013JC009517

Marsh, R., Desbruyères, D., Bamber, J. L., de Cuevas, B. A., Coward, A. C., & Aksenov, Y. (2010). Short-term impacts of enhanced greenland freshwater fluxes in an eddy-permitting ocean model. *Ocean Science*, *6*(3), 749–760. Retrieved from https://os.copernicus.org/articles/6/749/2010/ doi: 10.5194/os-6-749-2010

Martínez-Moreno, J., Hogg, A. M., Kiss, A. E., Constantinou, N. C., & Morrison, A. K. (2019). Kinetic energy of eddy-like features from sea surface altimetry. *Journal of Advances in Modeling Earth Systems*, *11*(10), 3090-3105. Retrieved from https://agupubs.onlinelibrary.wiley.com/doi/abs/10.1029/2019MS001769 doi: https://doi.org/10.1029/2019MS001769

Mastropole, D., Pickart, R. S., Valdimarsson, H., Våge, K., Jochumsen, K., & Girton, J. (2017). On the hydrography of denmark strait. *Journal of Geophysical Research: Oceans*, *122*(1), 306-321. Retrieved from https://agupubs.onlinelibrary.wiley.com/doi/abs/10.1002/2016JC012007 doi: 10.1002/2016JC012007

Mauritzen, C. (1996). Production of dense overflow waters feeding the north atlantic across the greenland-scotland ridge. part 1: Evidence for a revised circulation scheme. *Deep Sea Research Part I: Oceanographic Research Papers*, *43*(6), 769 - 806. Retrieved from http://www.sciencedirect.com/science/article/pii/0967063796000374 doi: http://dx.doi.org/10.1016/0967-0637(96)00037-4

Nøst, O. A., & Isachsen, P. E. (2003). The large-scale time-mean ocean circulation in the nordic seas and arctic ocean estimated from simplified dynamics. *Journal of Marine Research*, *61*(2), 175-210. Retrieved from https://www.ingentaconnect.com/content/jmr/jmr/2003/00000061/00000002/art00002 doi: doi:10.1357/002224003322005069

Nurser, A. J. G., & Bacon, S. (2014). The rossby radius in the arctic ocean. *Ocean Science*, *10*(6), 967–975. Retrieved from https://os.copernicus.org/articles/10/967/2014/ doi: 10.5194/os-10-967-2014

Oberhuber, J. M. (1993). Simulation of the atlantic circulation with a coupled sea ice-mixed layer-isopycnal general circulation model. part i: Model description. *Journal of Physical Oceanography*, *23*(5), 808-829. Retrieved from http://dx.doi.org/10.1175/1520-0485(1993)023<0808:SOTACW>2.0.CO;2 doi: 10.1175/1520-0485(1993)023⟨0808:SOTACW⟩2.0.CO;2

Olsson, K. A., Jeansson, E., Tanhua, T., & Gascard, J.-C. (2005). The east greenland current studied with cfcs and released sulphur hexafluoride. *Journal of Marine Systems*, *55*(1), 77 - 95. Retrieved from http://www.sciencedirect.com/science/article/pii/S0924796304002568 doi: https://doi.org/10.1016/j.jmarsys.2004.07.019

Rudels, B., Björk, G., Nilsson, J., Winsor, P., Lake, I., & Nohr, C. (2005). The interaction between waters from the arctic ocean and the nordic seas north of fram strait and along the east greenland current: results from the arctic ocean-02 oden expedition. *Journal of Marine Systems*, *55*(1), 1 - 30. Retrieved from http://www.sciencedirect.com/science/article/pii/S0924796304002015 doi: https://doi.org/10.1016/j.jmarsys.2004.06.008

Schauer, U., & Losch, M. (2019). "freshwater" in the ocean is not a useful parameter in climate research. *Journal of Physical Oceanography*, *49*(9), 2309-2321. Retrieved from https://doi.org/10.1175/JPO-D-19-0102.1 doi: 10.1175/JPO-D-19-0102.1

Schmith, T., Olsen, S. M., Ringgaard, I. M., & May, W. (2018). Limited predictability of extreme decadal changes in the arctic ocean freshwater content. *Climate*

Dynamics, *51*(9), 3927-3942. Retrieved from https://doi.org/10.1007/s00382-018-4120-8 doi: 10.1007/s00382-018-4120-8

Schulze Chretien, L. M., & Frajka-Williams, E. (2018). Wind-driven transport of fresh shelf water into the upper 30 m of the labrador sea. *Ocean Science*, *14*(5), 1247–1264. Retrieved from https://os.copernicus.org/articles/14/1247/2018/ doi: 10.5194/os-14-1247-2018

Selyuzhenok, V., Bashmachnikov, I., Ricker, R., Vesman, A., & Bobylev, L. (2020). Sea ice volume variability and water temperature in the greenland sea. *The Cryosphere*, *14*(2), 477-495. Retrieved from https://www.the-cryosphere.net/14/477/2020/ doi: 10.5194/tc-14-477-2020

Sgubin, G., Swingedouw, D., Drijfhout, S., Mary, Y., & Bennabi, A. (2017). Abrupt cooling over the north atlantic in modern climate models. *Nature Communications*, *8*(1), 14375. doi: 10.1038/ncomms14375

Simmons, H. L., Jayne, S. R., Laurent, L. C. S., & Weaver, A. J. (2004). Tidally driven mixing in a numerical model of the ocean general circulation. *Ocean Modelling*, *6*(3-4), 245-263. Retrieved from http://www.sciencedirect.com/science/article/pii/S1463500303000118 doi: http://dx.doi.org/10.1016/S1463-5003(03)00011-8

Smedsrud, L. H., Sorteberg, A., & Kloster, K. (2008). Recent and future changes of the arctic sea-ice cover. *Geophys. Res. Lett.*, *35*.

Spall, M. A., Almansi, M., Huang, J., Haine, T. W., & Pickart, R. S. (2021). Lateral redistribution of heat and salt in the nordic seas. *Progress in Oceanography*, *196*, 102609. Retrieved from https://www.sciencedirect.com/science/article/pii/S0079661121000963 doi: https://doi.org/10.1016/j.pocean.2021.102609

Sutherland, D. A., & Pickart, R. S. (2008). The east greenland coastal current: Structure, variability, and forcing. *Progress in Oceanography*, *78*(1), 58 - 77. Retrieved from http://www.sciencedirect.com/science/article/pii/S0079661108000864 doi: https://doi.org/10.1016/j.pocean.2007.09.006

Swift, J. H., & Aagaard, K. (1981). Seasonal transitions and water mass formation in the iceland and greenland seas. *Deep Sea Research Part A. Oceanographic Research Papers*, *28*(10), 1107 - 1129. Retrieved from http://www.sciencedirect.com/science/article/pii/0198014981900509 doi: https://doi.org/10.1016/0198-0149(81)90050-9

Trodahl, M., & Isachsen, P. E. (2018). Topographic influence on baroclinic instability and the mesoscale eddy field in the northern north atlantic ocean and the nordic seas. *Journal of Physical Oceanography*, *48*(11), 2593 - 2607. Retrieved from https://journals.ametsoc.org/view/journals/phoc/48/11/jpo-d-17-0220.1.xml doi: 10.1175/JPO-D-17-0220.1

Våge, K., Moore, G., Jónsson, S., & Valdimarsson, H. (2015). Water mass transformation in the iceland sea. *Deep Sea Research Part I: Oceanographic Research Papers*, *101*, 98 - 109. Retrieved from http://www.sciencedirect.com/science/article/pii/S0967063715000680 doi: https://doi.org/10.1016/j.dsr.2015.04.001

Våge, K., Papritz, L., Håvik, L., Spall, M. A., & Moore, G. W. K. (2018). Ocean convection linked to the recent ice edge retreat along east greenland. *Nature Communications*, *9*(1), 1287. Retrieved from https://doi.org/10.1038/s41467-018-03468-6 doi: 10.1038/s41467-018-03468-6

Venegas, S. A., & Mysak, L. A. (2000). Is there a dominant timescale of natural climate variability in the arctic? *Journal of Climate*, *13*(19), 3412-3434. Retrieved from https://doi.org/10.1175/1520-0442(2000)013<3412:ITADTO>2.0.CO;2 doi: 10.1175/1520-0442(2000)013⟨3412:ITADTO⟩2.0.CO;2

Vinje, T. (2001). Fram strait ice fluxes and atmospheric circulation: 1950–2000. *Journal of Climate*, *14*(16), 3508-3517. doi: 10.1175/1520-0442(2001)014⟨3508:FSIFAA⟩2.0.CO;2

Voet, G., Quadfasel, D., Mork, K. A., & Søiland, H. (2010). The mid-depth circulation of the nordic seas derived from profiling float observations. *Tellus A*, *62*(4), 516-529. Retrieved from https://onlinelibrary.wiley.com/doi/abs/10.1111/j.1600-0870.2010.00444.x doi: 10.1111/j.1600-0870.2010.00444.x

Weijer, W., Cheng, W., Garuba, O. A., Hu, A., & Nadiga, B. T. (2020). Cmip6 models predict significant 21st century decline of the atlantic meridional overturning circulation. *Geophysical Research Letters*, *47*(12), e2019GL086075. Retrieved from https://agupubs.onlinelibrary.wiley.com/doi/abs/10.1029/2019GL086075 (e2019GL086075 10.1029/2019GL086075) doi: https://doi.org/10.1029/2019GL086075

Zamani, B., Krumpen, T., Smedsrud, L. H., & Gerdes, R. (2019). Fram strait sea ice export affected by thinning: comparing high-resolution simulations and observations. *Climate Dynamics*, *53*(5), 3257-3270. Retrieved from https://doi.org/10.1007/s00382-019-04699-z doi: 10.1007/s00382-019-04699-z

Additional references

IPCC, 2019: IPCC Special Report on the Ocean and Cryosphere in a Changing Climate [H.-O. Pörtner, D.C. Roberts, V. Masson-Delmotte, P. Zhai, M. Tignor, E. Poloczanska, K. Mintenbeck, A. Alegría, M. Nicolai, A. Okem, J. Petzold, B. Rama, N.M. Weyer (eds.)].

Helland-Hansen, B., and F. Nansen, 1909: The Norwegian Sea, its physical oceanography based upon the Norwegian Researches 1900-1904. Report on Norwegian and Marine Investigations, 2, 390 pp.

Large WG, Yeager S (2004) Diurnal to decadal global forcing for ocean and sea-ice models: The data sets and flux climatologies. NCAR Technical Note NCAR/TN-460+STR. https://doi.org/10.5065/D6KK98Q6

Smagorinsky, J., Large eddy simulation of complex engineering and geophysical flows, in Evolution of Physical Oceanography, edited by B. Galperin, and S. A. Orszag, pp. 3-36. Cambridge University Press, 1993.

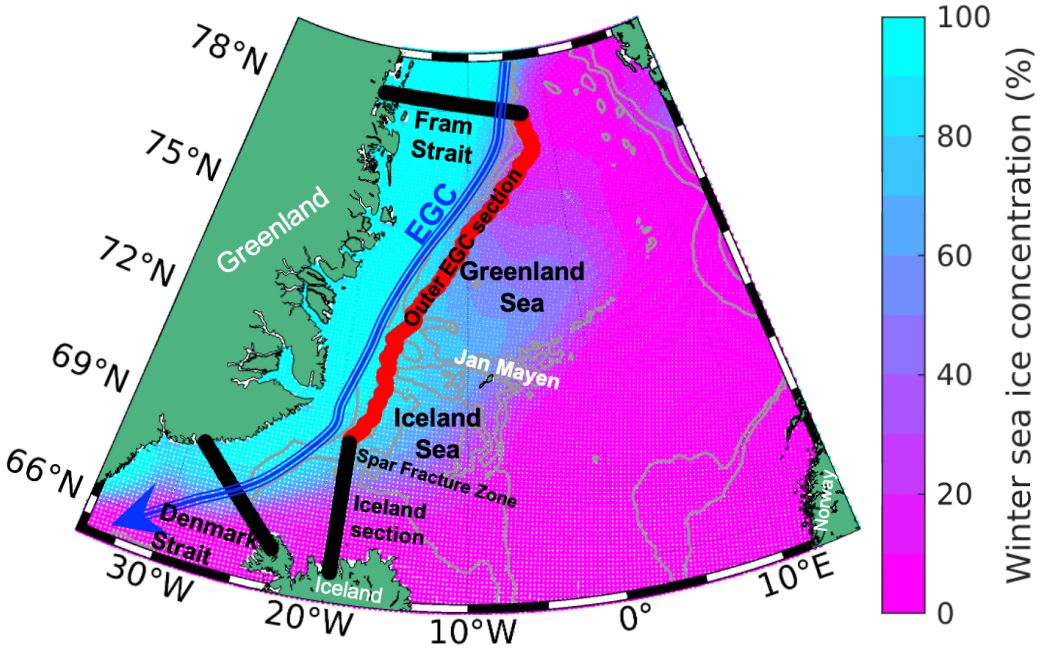

Figure 1. The focus region of this study is the western Nordic Seas; encompassing the East Greenland Current (EGC), carrying freshwater and sea ice southward, and the Greenland and Iceland Seas. The three sections marked in black are referred to in the text as the Fram Strait, the Denmark Strait and the Iceland section. The section in red is aligned with the EGC but outside of the main core, i.e., outside the location of maximum velocities. The colour shading is the mean simulated winter (Jan-Feb-Mar) sea ice concentration for the period 1973-2004 from the forced global ocean-ice model used in this study. The depth contours are 1200 and 2000m (thin grey lines).

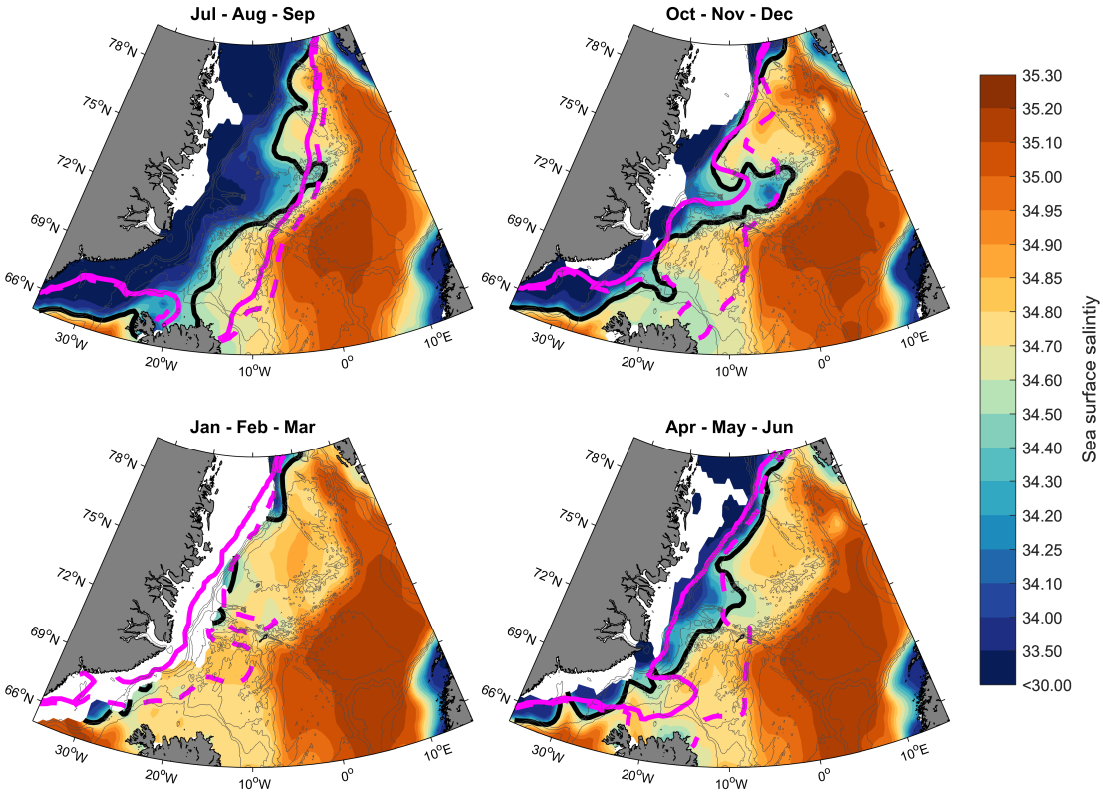

Figure 2. Seasonal variability in surface salinity (averaged over the upper 50m) based on observations (Huang et al., 2020) for the period 1986-2016. The solid black line shows the S=34.5 isohaline, which marks the Polar Front. The solid (dashed) magenta lines show the simulated S=34.3 (S=34.5) isohaline for the period 1986-2004. The depth contours are 500, 1000, 1500, 2000, 3000, and 4000m (thin grey lines).

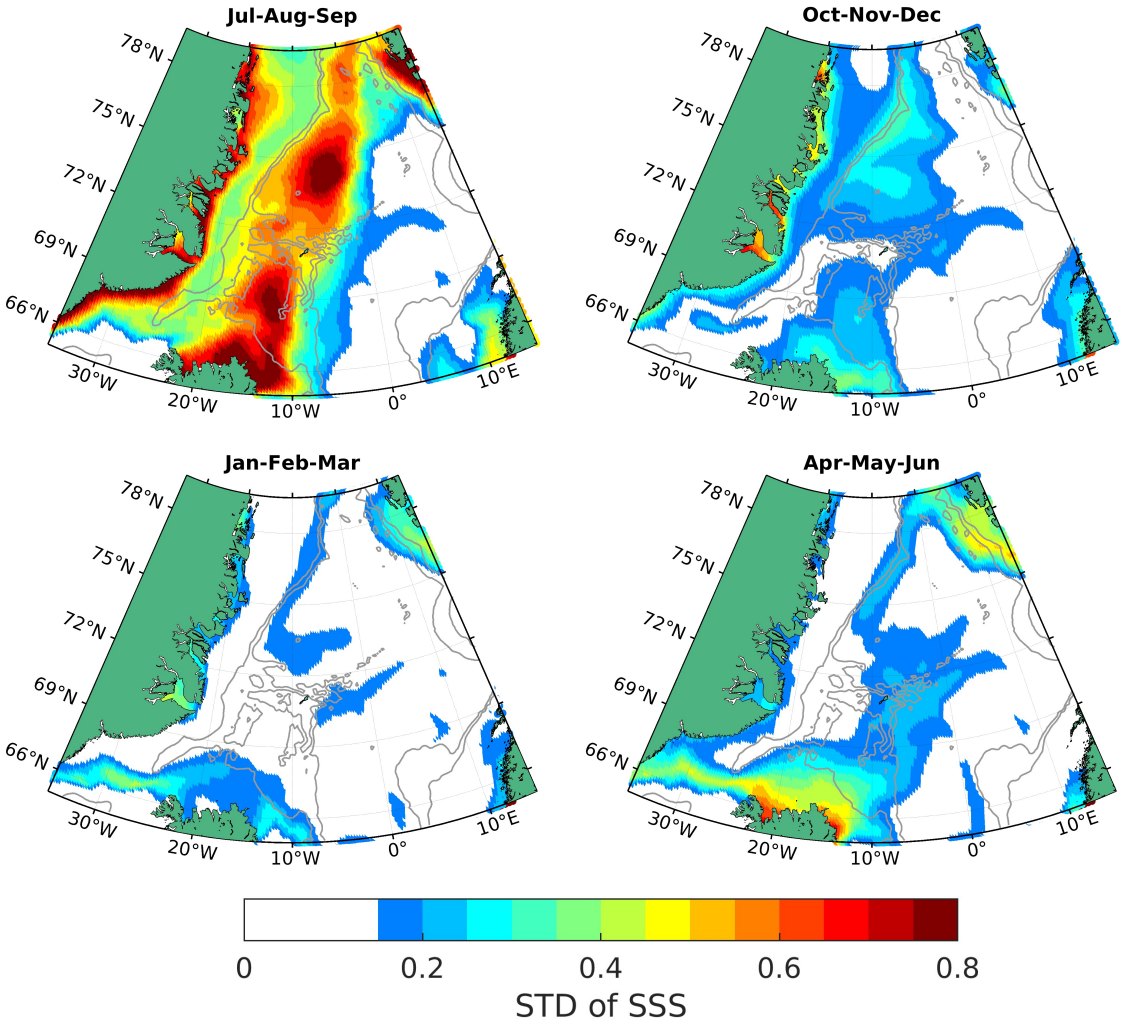

Figure 3. Standard deviation of simulated Sea Surface Salinity (SSS) in NorESM for the period 1973-2004 for four different seasons (all time series are detrended). The depth contours are 1200 and 2000m (thin grey lines).

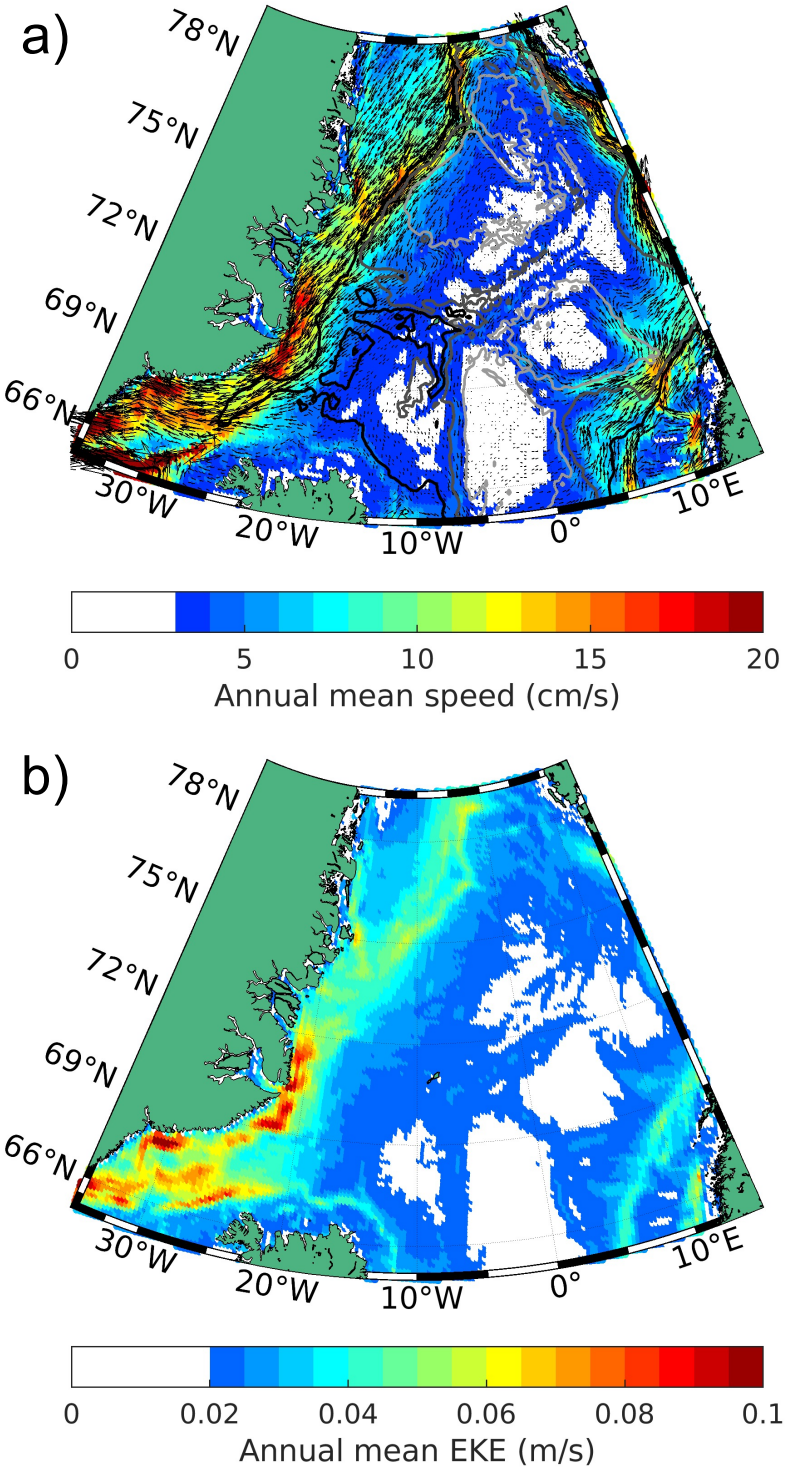

Figure 4. a) Simulated mixed-layer velocity in NorESM, showing the annual average over the period 1973-2004. The direction of the currents is shown by the black arrows and the mean speed is shown by colour. The simulated East Greenland Current is shown as a strong southward current in the westernmost part of the Nordic Seas. The depth contours are 1200 (black line), 2000, and 3000m (grey lines). b) Simulated Eddy Kinetic Energy (EKE) using mixed layer velocities.

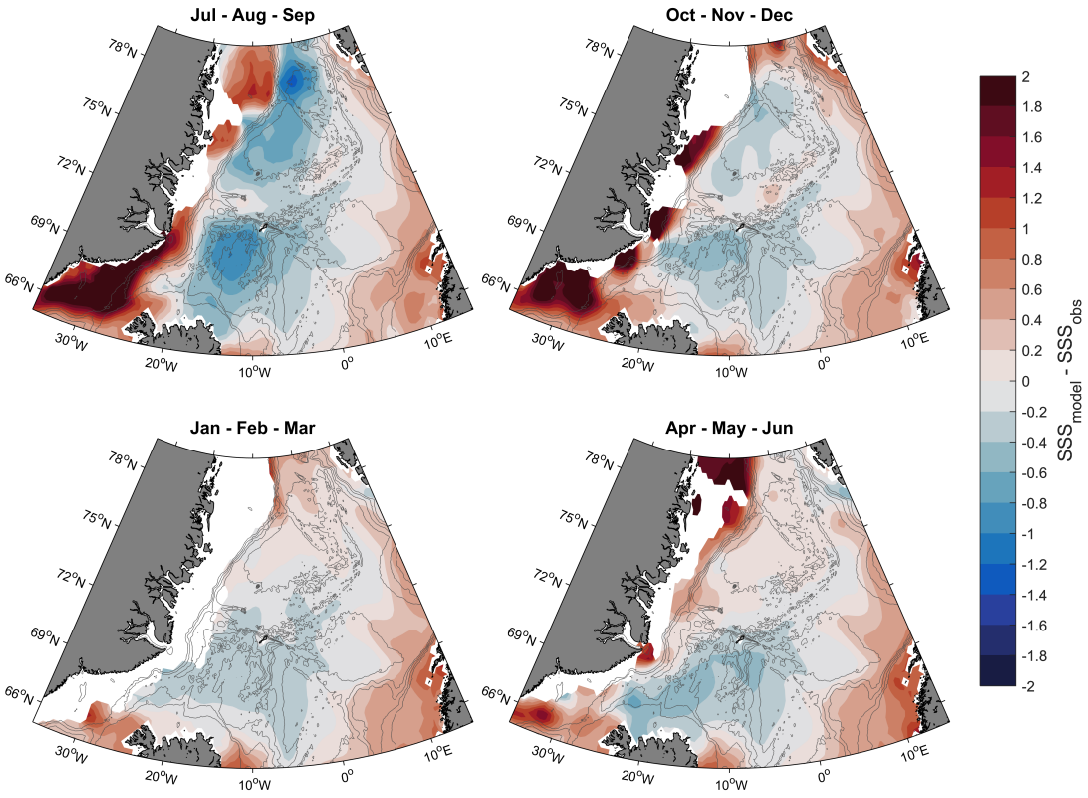

Figure 5. The seasonal differences between observed and simulated surface salinity (model minus observations). The depth contours are 500, 1000, 1500, 2000, 3000, and 4000m (thin grey lines).

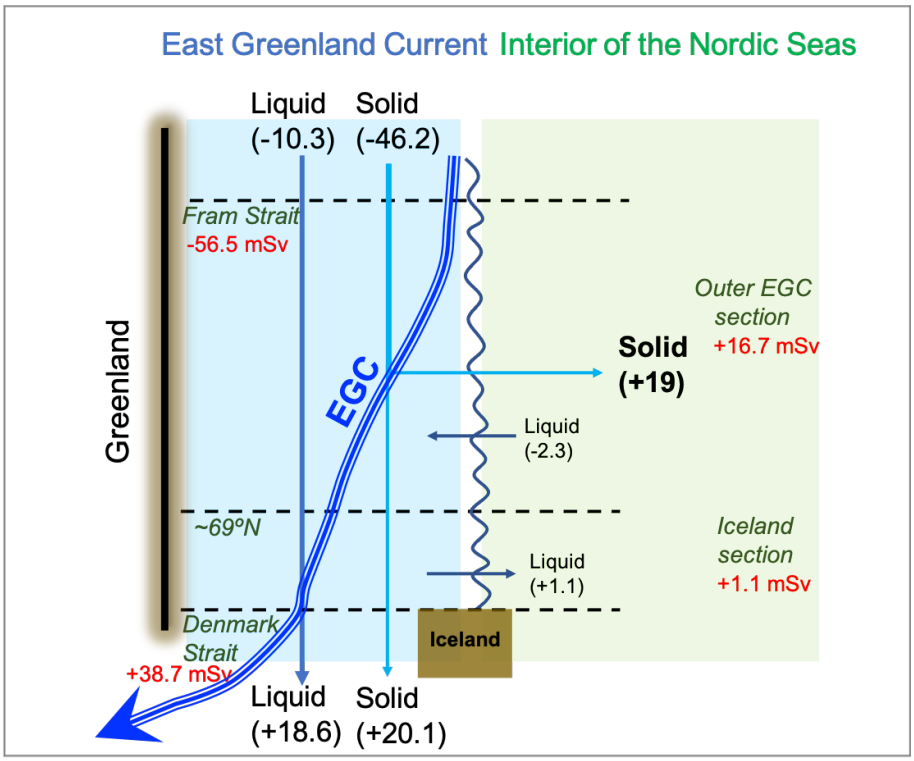

Figure 6. Schematic of the freshwater budget in the model simulation for the region enclosed by the four sections: Fram Strait, Denmark Strait, outer EGC section, and Iceland section (the two latter are separated at about 69°N). The annual mean liquid and solid freshwater transports for the period 1973-2004 are shown in black (numbers in mSv), and the total freshwater transport (liquid + solid) across each section is given by the red numbers. The schematic is adopted after Dodd et al. (2009).

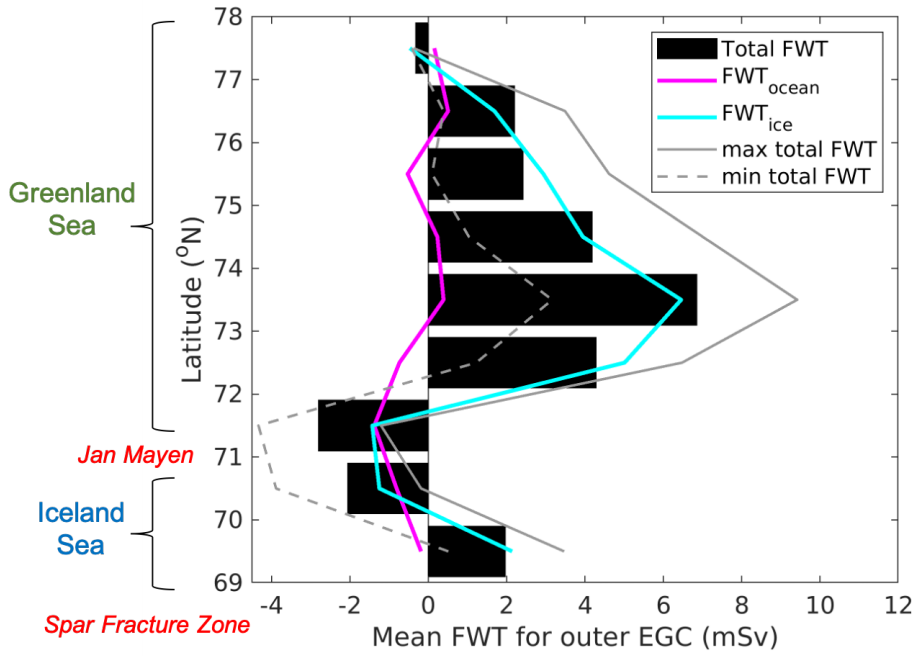

Figure 7. The total simulated freshwater transport (FWT) across the outer EGC section, as a function of latitude, given as the annual mean for the period 1973-2004. Positive values mean that there is a total FWT towards the east (the interior of the Nordic Seas). Negative values mean that there is a total FWT towards the west (the Greenland shelf). The liquid freshwater transport (FWTocean) and solid freshwater transport (FWTice) are also shown. In addition, the latitudinal distribution of the total FWT for two different cases are shown (see the red and blue points in Fig. 13). The approximate locations for the Greenland and Iceland Seas are indicated, separated by Jan Mayen. The outer EGC section ends just north of the Spar Fracture Zone.

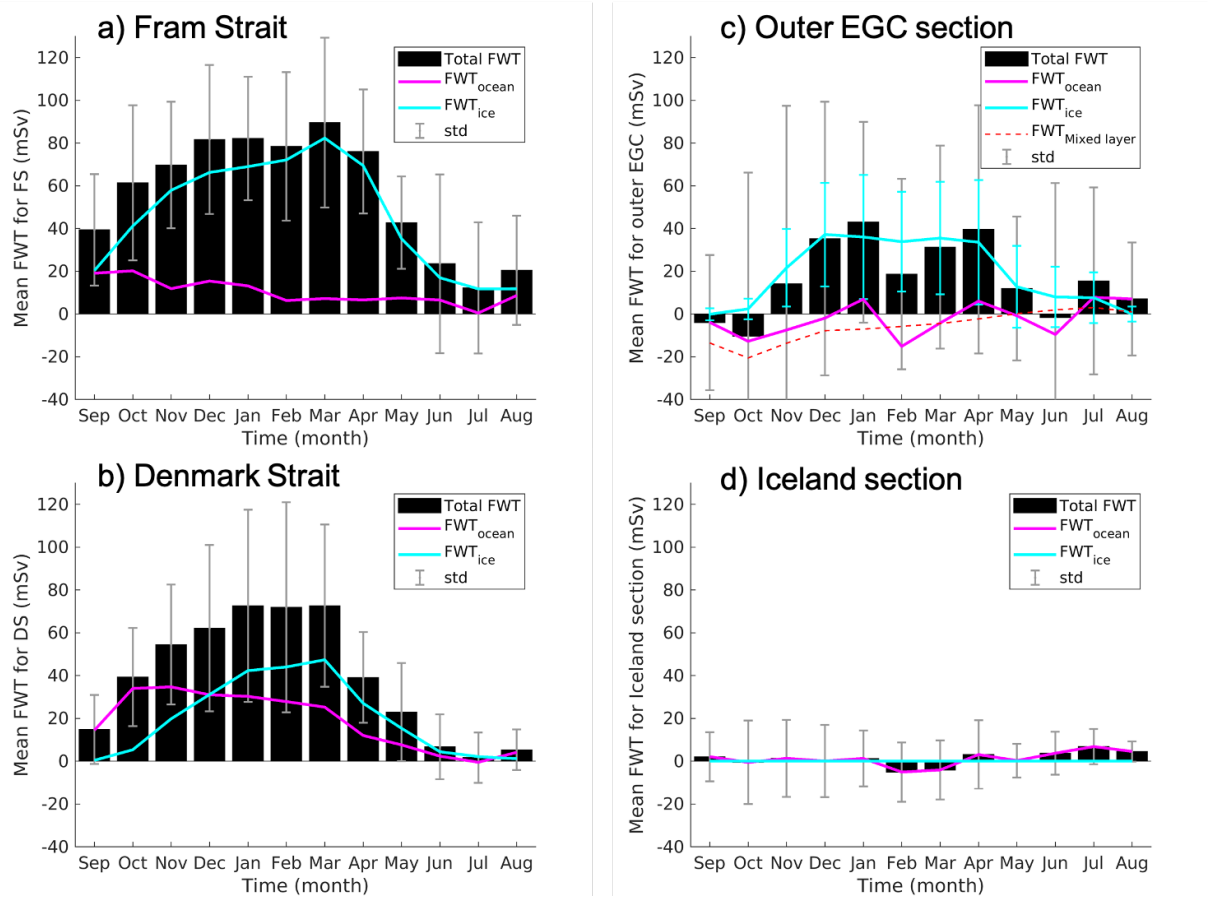

Figure 8. Mean seasonal cycles of simulated liquid freshwater transport (FWTocean; magenta curves) and simulated solid freshwater transport (FWTice; light blue curves) for the period 1973-2004. The total FWT is shown as black bars. The FWT is shown for all four sections in Fig. 1; a) Fram Strait, b) Denmark Strait, c) outer EGC section, and d) Iceland section. Positive FWT across Denmark Strait, outer EGC, and Iceland section means that the transport is out of the closed domain in Fig. 1. Note that the sign of the FWT across Fram Strait is reversed, i.e., positive FWT across Fram Strait means that the transport is into the closed domain. The standard deviation (std) of the detrended time series for the period 1973-2004 is added on the black bars (grey vertical lines). In c), the std is also shown for FWTice (light blue vertical lines), and the red dashed curve shows the FWT in the mixed layer.

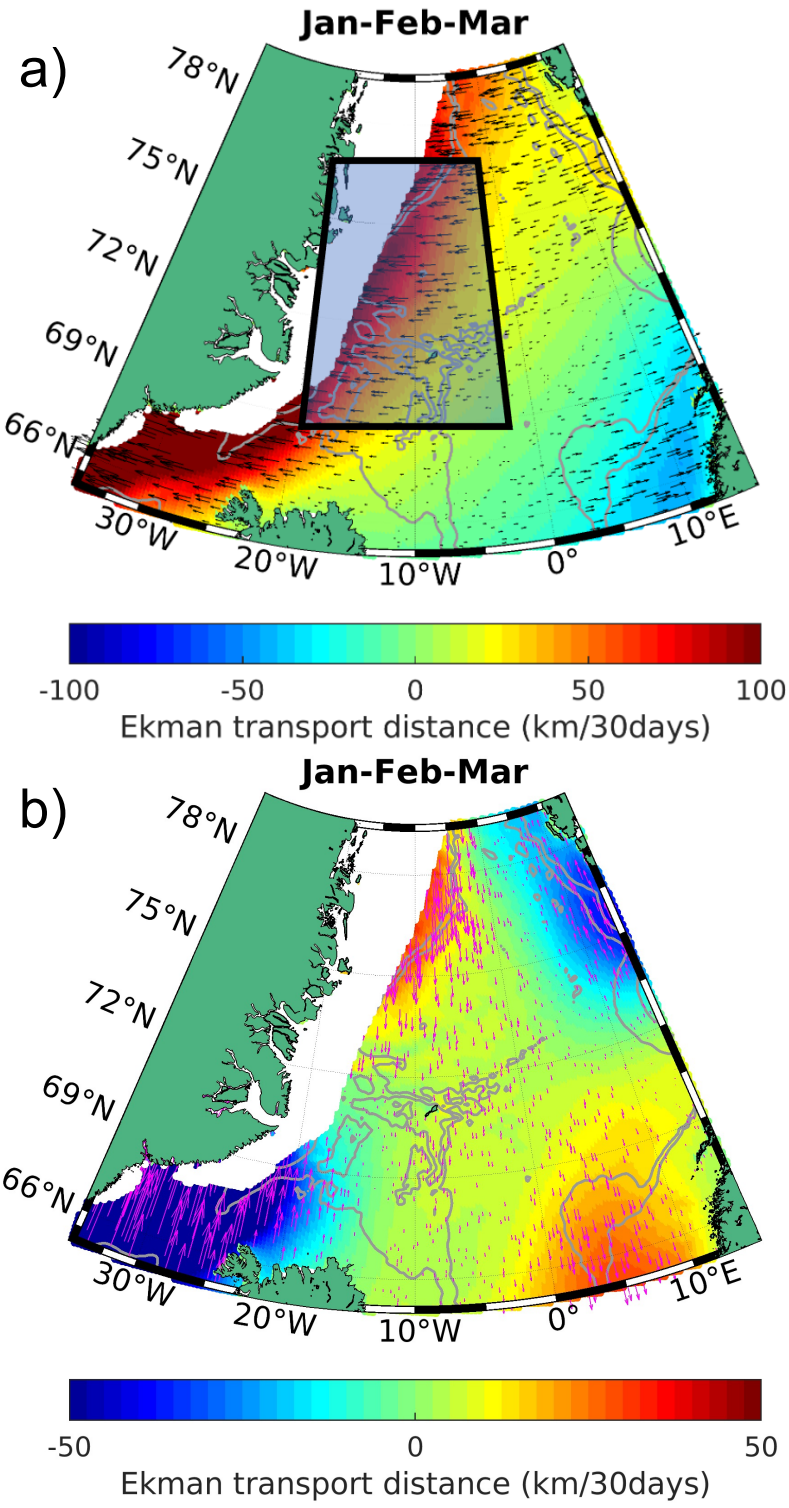

Figure 9. The simulated Ekman transport distance in winter for the period 1973-2004, where the magnitude is shown by colour. The direction of a) the zonal component (black) and b) the meridional component (magenta) of the Ekman transport is shown by the arrows. In the western Nordic Seas (defined by the box), the zonal component is westward and the meridional component is southward. The depth contours are 1200 and 2000m (thin grey lines). The white region is the area where the sea ice concentration is larger than 90%. Note the difference in the scale of the magnitude in a) and b).

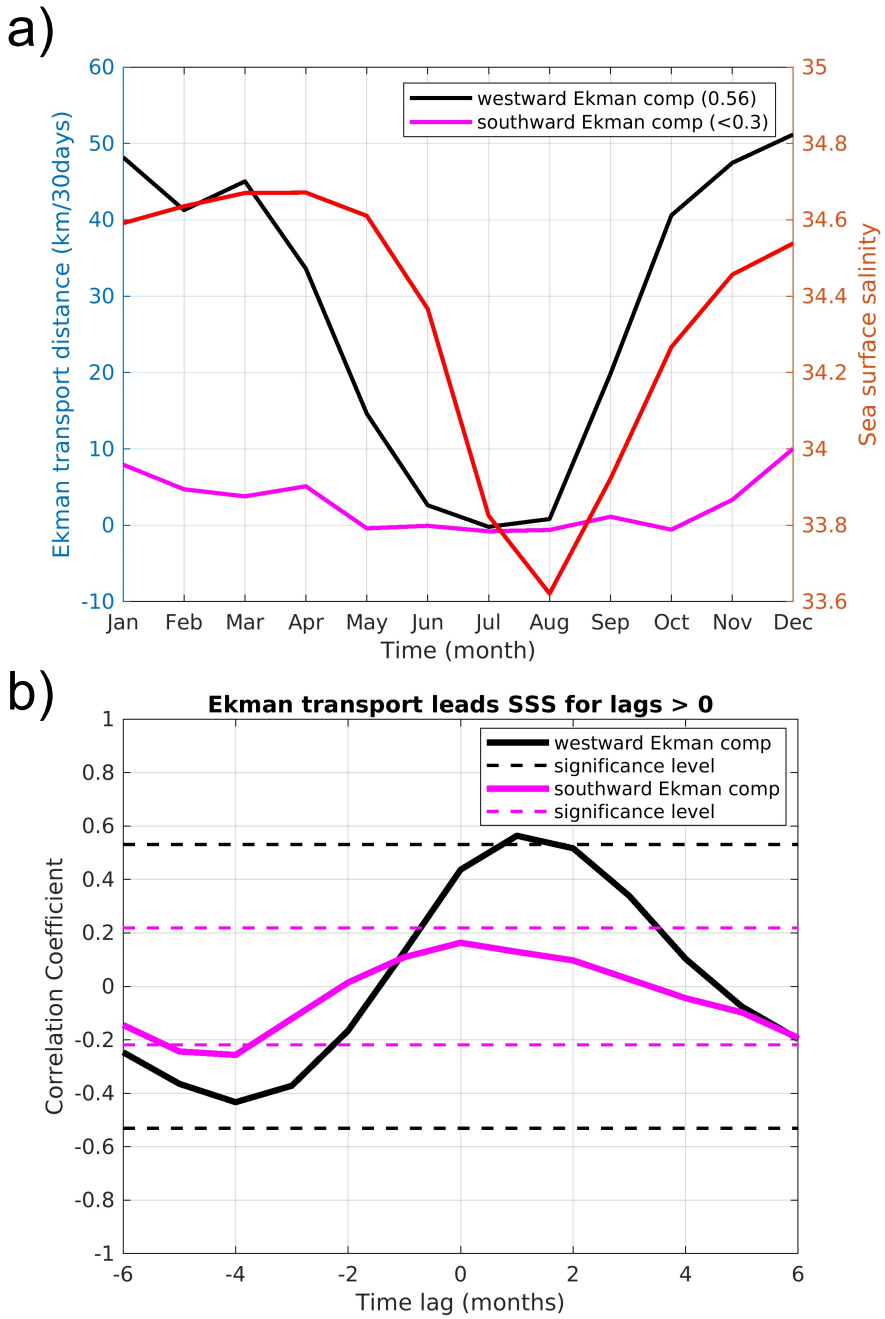

Figure 10. a) Mean seasonal cycles of simulated variables in the western Nordic Seas (averaged over the box domain in Fig. 9a). The scale for Ekman transport distance is shown on the left y-axis, whereas the scale for Sea Surface Salinity (SSS; red curve) is shown on the right y-axis. The numbers in parenthesis are the maximum correlation with SSS. b) Cross-correlation between SSS and Ekman transport distance (for each component separately), where we use all months for the full time period 1973-2004 (32*12 points). The dashed lines mark the 95% significance level.

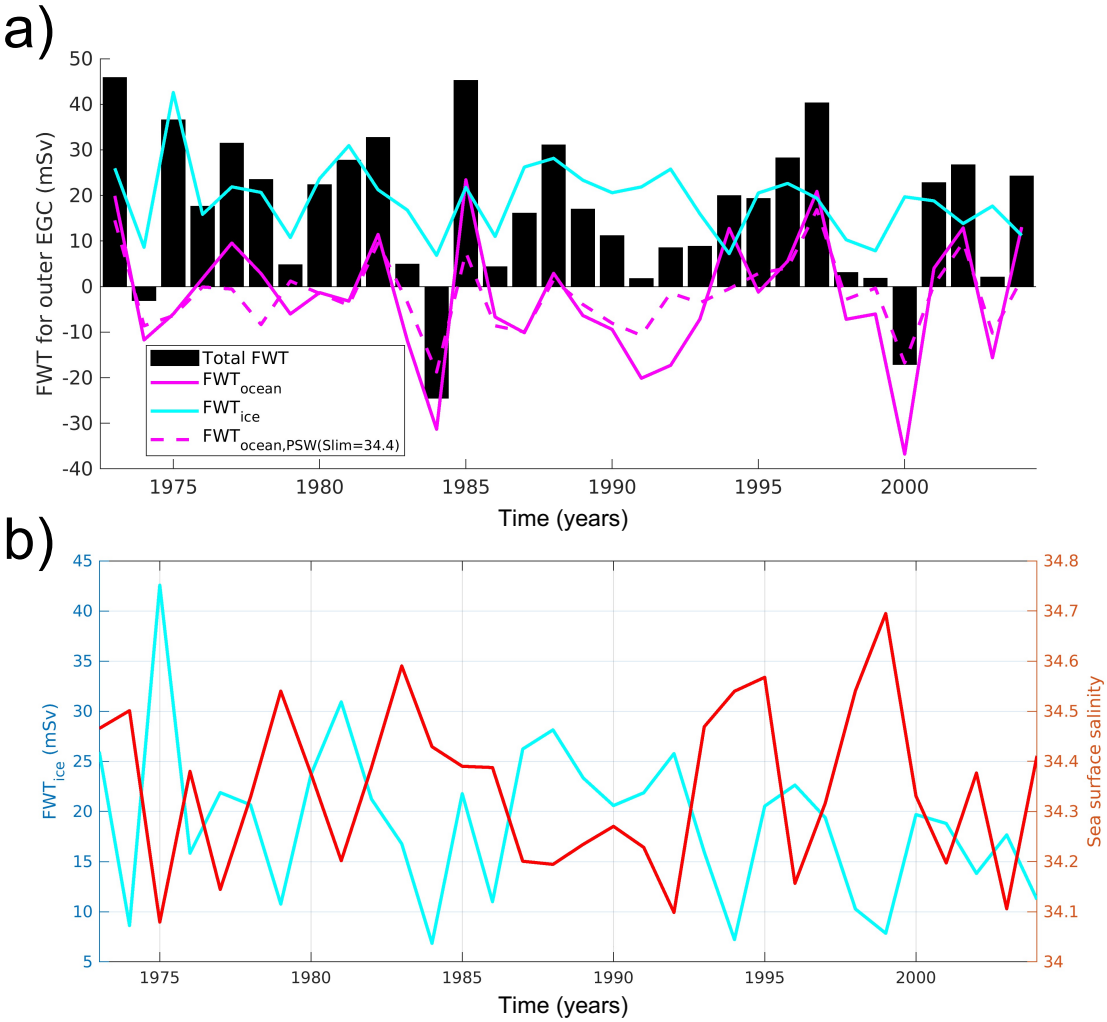

Figure 11. a) The annual mean total freshwater transport (FWT) across the outer EGC section in the model simulation. The liquid freshwater transport (FWTocean) and solid freshwater transport (FWTice) are also shown. The FWTocean using a salinity limit of 34.4 is also shown (dashed line), in order to give an estimate of the liquid freshwater transport in Polar Surface Water (PSW). Positive values mean that the transport is out of the closed domain shown in Fig. 1. b) Temporal evolution of FWTice and SSS in the western Nordic Seas (the latter is averaged over the box domain in Fig. 9a). The scale for FWTice is shown on the left y-axis (blue), whereas the scale for SSS is shown on the right y-axis (red).

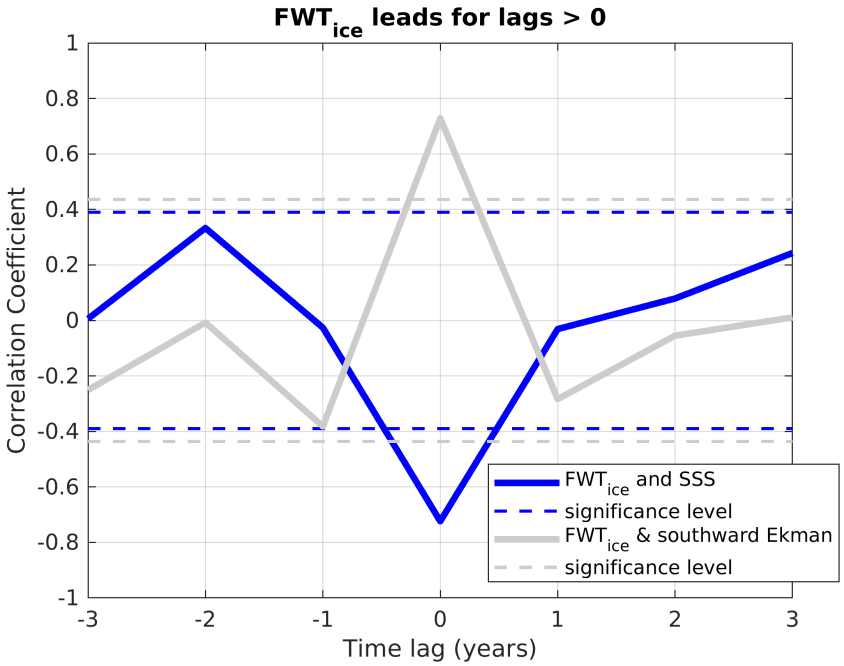

Figure 12. Cross-correlation between the solid freshwater transport (FWTice) across the outer EGC section and SSS in the western Nordic Seas (blue curve), and cross-correlation between FWTice and the southward Ekman transport distance in the western Nordic Seas (gray curve). We use annual means for the period 1973-2004. The dashed lines mark the 95% significance level.

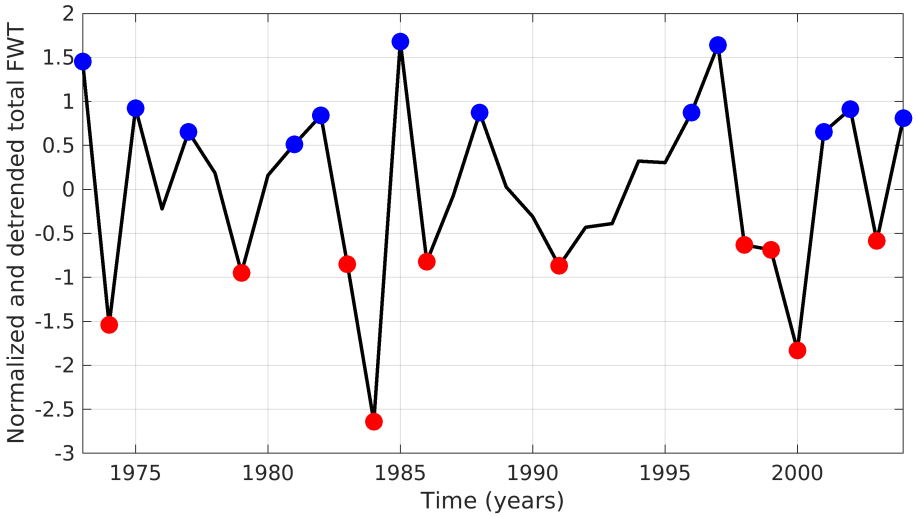

Figure 13. Time series of the normalized and detrended total freshwater transport (FWT) across the outer EGC section in the model simulation. Composite analysis is done for years with values above (below) the value 0.5, marked by blue (red) circles. The years with blue circles are those with high FWT into the interior of the Nordic Seas, and years with red circles are those with low FWT into the interior.

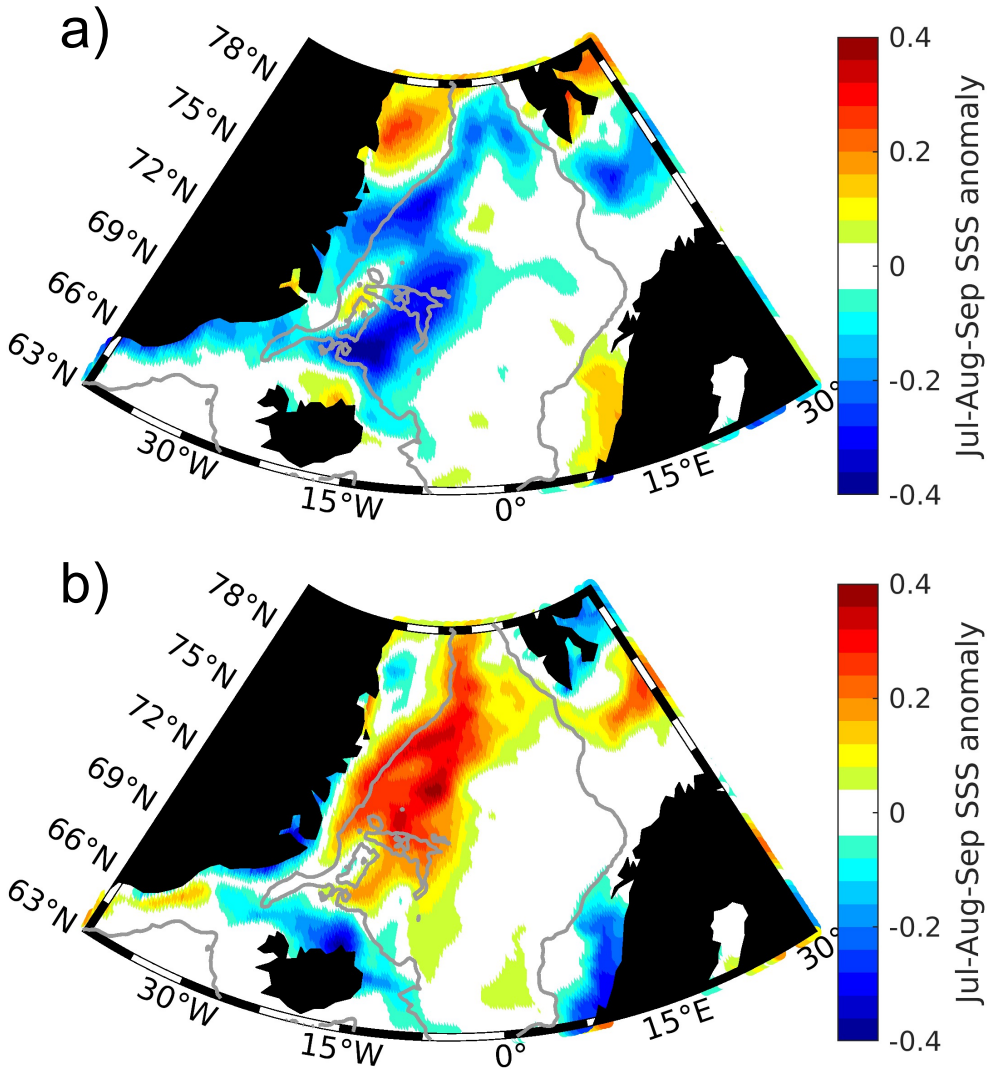

Figure 14. Composites of simulated SSS anomalies in late summer (Jul-Sep). a) and b) show anomalies associated with the years marked by blue and red circles, respectively, in Fig. 13. The thin grey lines show the 1200m isobath.